Optimal Deployment of Air Vehicle as Communication Relay for Multiple Ground Vehicles

Juan David Pabon Arias
West Virginia University, jdp00025@mix.wvu.edu

Optimal Deployment of Air Vehicle as Communication Relay for Multiple Ground Vehicles

Juan David Pabon Arias

Thesis submitted to the

Benjamin M. Statler College of Engineering and Mineral Resources

at West Virginia University

in partial fulfillment of the requirements for the degree of

Master of Science

in

Aerospace Engineering

Xi Yu, Ph.D., Chair

Matthew C. Valenti, Ph.D.

Guilherme A. S. Pereira, Ph.D.

Mechanical and Aerospace Engineering Department

Morgantown, West Virginia

2023

Keywords: Multiple Vehicles, Line-of-Sight, Air-Aided Communication

Abstract

Optimal Deployment of Air Vehicle as Communication Relay for Multiple Ground Vehicles

Juan David Pabon Arias

Heterogeneous teams of both air and ground mobile vehicles can combine the advantages of mobility, sensing capability, and operation time when performing complex tasks. However, when ground vehicles operate in cluttered environments with randomized obstacles, they may experience line of sight (LoS) obstructions and loss of communication due to those obstacles. To mitigate this issue, an airborne relay can be positioned in the vicinity of the ground vehicles to aid communication by establishing two-hop communication links between the vehicles.

This thesis develops an analytical framework to calculate the probability of spanning a two-hop communication between a pair of ground vehicles deployed in a task space with obstacles at random locations and with random heights (i.e., a Poisson Forest) using an airborne relay at any location near the ground vehicles. It allows to provide the main result, the optimization of the airborne relay's location in scenarios involving multiple ground vehicles.

By considering the locations and heights of the ground vehicles and the airborne relay, the distance-dependent critical height describing the required height of an obstacle to block the LoS is established. To account for the dependence on distance, the blocking is modeled as an inhomogeneous Poisson point process, and the LoS probability is its void probability. When pairwise communication links are considered, the throughput (metric depending on the LoS probability and channel capacity) is used to determine when to deploy the airborne relay, and, when the airborne relay is deployed, its optimal 3-D location.

When multiple ground vehicles are considered, the throughput of the links and the layout of the communication network formed by the vehicles are used to compute the optimal positioning of the airborne relay, thus enhancing the overall throughput and connectivity of the network. The results are illustrated considering two obstacle height distributions: uniform and truncated Gaussian.

Acknowledgments

I would like to show my sincere appreciation to my research Advisor, Dr. Xi Yu. Her expertise and knowledge in the field of multi-agent systems were crucial to the development of this research. Also, I would like to thank Dr. Matthew Valenti for his support in the field of communication systems and the support along the development of the research.

Furthermore, I would like to recognize my committee member Dr. Guilherme Pereira for sharing the FARO Lab with the research group in which I was involved, including us in their seminars, and providing support and advice for the projects in which we were working.

I am very fortunate to have completed this academic journey with my wife Paula Lozano. Her never-ending support over these years provided me the motivation to continue this journey even in the most difficult situations.

Contents

List of Abbreviations

CDF Cumulative Distribution Function

erf Error Function

LoS Line of Sight

PLoS Probability of having Line of Sight

PPP Poisson Point Process

SNR Signal-to-Noise Ratio

List of Figures

Chapter 1

Introduction

1.1 Motivation

The deployment of coordinated autonomous mobile agents, including both ground and air vehicles, has gained interest across a variety of applications, such as long-term monitoring and post-disaster rescue operations in large and intricate task environments like urban areas and forests [1–6]. This heterogeneity of mobile agents presents a multifaceted advantage: air vehicles offer rapid mobility and extensive sensing coverage, while ground vehicles deliver precise sensing capabilities and enduring operational time [7].

In various scenarios, air vehicles play diverse roles, from acting as communication relays [8] to providing remote sensing of battlegrounds [9]. The strategic placement of these air vehicles is critical, as it must ensure continuous connectivity with the appropriate sets of ground vehicles.

Efficient coordination between these vehicles often necessitates the transmission of substantial data volumes, particularly between air and ground vehicles, to achieve mission success [10]. Modern communication technologies leverage high data transmission rates, often employing short wavelengths, such as mmWave frequencies or visible light, to accomplish this. However, these shorter wavelengths are prone to obstruction, impacting line of sight (LoS) connectivity [11]. In task spaces of the real world, obstacles of varying shapes, heights, and positions can block the LoS paths. Such blockages may also impede essential functions like localization and mapping, which rely on cameras and lidar sensors [12, 13].

Mobile agents possess the advantage of repositioning themselves to reestablish LoS paths when obstructed. This capability is highly advantageous, assuming detailed obstacle maps are available. However, in practice, relying solely on pre-existing maps for path planning and obstacle avoidance is often infeasible. Dynamic factors like civilian activities, military operations, disasters, or terrain transformations can make such maps obsolete. Additionally, in complex environments like dense forests, cataloging and accurately representing all obstacles can be a challenging task [14].

To address these limitations associated with fixed deterministic maps, an alternative approach models obstacles in urban and forested areas as stochastically distributed. For instance, previous works [15–17] have modeled urban buildings using Manhattan Poisson line processes with randomized heights, while forested areas have been represented with randomly located trees [18–20] and random tree heights [21–23]. A forest-like cluttered environment is described through a Poisson point process, often referred to as a *Poisson Forest*.

In such stochastic obstacle environments, the probability of an obstructed path between two vehicles, and conversely, the LoS probability, can be computed. Our prior works [24, 25] demonstrated the benefits of deploying an air vehicle as a communication relay of two ground vehicles in a Poisson Forest, focusing on deriving the LoS probability and throughput as well as calculating the air vehicle's positions producing fixed values of these metrics. However, in those works, it was assumed that the air vehicle was aiding the communication of only two ground vehicles. In some cases, aiding the communication of more than two ground vehicles could be required.

1.2 Objectives

Our prior works [24,25] presented the benefits of deploying an air vehicle as a communication relay of two ground vehicles in a Poisson Forest. In these works, a theoretical framework was developed to compute the LoS probability and the throughput for the positions in which the air vehicle is deployed. Also, these works determined the location in which it is better to implement a direct-hop communication between ground vehicles or a two-hop communication using the airborne relay.

The main objective of this thesis is to develop a theoretical framework that allows us to determine the optimal position of the air vehicle when it is used as an airborne relay for multiple ground vehicles. The metric used to evaluate optimal position is the throughput which balances the LoS probability and the signal loss due to the the transmission distance.

To achieve our main objective, this thesis achieves the following objectives:

- Modeling the positions and heights of the random obstacles and determining what obstacles are a blockage for the LoS.
- Computing the LoS for different height distributions (uniform and truncated Gaussian distributions).
- Defining a metric to evaluate the quality of the communication of a team of ground-air-ground vehicles while accounting for the LoS probability and loss signal due to the transmission distance.
- Defining a metric to evaluate the quality of the communication in a network of multiple ground vehicles and one air vehicle.

The following chapters of this thesis show how each of the previous objectives is achieved and how achieving them allows us to achieve the main objective of the thesis: determining the optimal position of the air vehicle when it is used as an airborne relay for multiple ground vehicles.

1.3 Contributions

This thesis extends the results presented in [24, 25], addressing the issue of identifying optimal locations for the air vehicle when teams of multiple ground vehicles are considered. Our approach aims to locate the air vehicle based on determining first for the two ground vehicles case, the distances at which is better to rely on direct-hop communication between ground vehicles and after which distance it is better to rely on two-hop communication using the air vehicle as an airborne relay. When multiple ground vehicles are considered, it is used to determine what type of link is better for each pair of vehicles (one-hop or two-hop links). Also, finding the positions in the 3-D space in which the air vehicle provides constant values of LoS probability or throughput allows determining surfaces in 3-D space defining a volume where LoS probability or throughput is guaranteed. By constraining the air vehicle's location within this volume, desired performances can be obtained. These regions are useful to determine the regions in which positing the air vehicle will improve the communication of several pairs of ground vehicles.

Beyond the consideration of locations with constant LoS probability and throughput for two ground vehicles, the thesis uses the throughput of the pairwise links between ground vehicles to deal with the issue of where to deploy the airborne relay when multiple ground vehicles are considered. First, the throughput for each pairwise link and the overall throughput of the network formed by the vehicles are calculated. Then, the connectivity of the network and the overall throughput of the links is used to define the metric describing the overall quality of the communication. This metric is used to find the optimal position to deploy the airborne relay to aid the communication of multiple ground vehicles. In that position, the value of such metric is maximized.

1.4 Thesis Organization

The remainder of this thesis is organized as follows. Chapter 2 calculates the probability of having LoS in a Poisson forest. Chapter 3 provides the analysis and closed-form expressions for calculating the LoS probability and throughput when two ground vehicles are considered. Chapter 4 calculates the positions of an airborne relay that produces constant values of LoS probability or throughput for the two ground vehicles case. Chapter 5 extends the results of the previous chapters to analyze the case in which more than two ground vehicles are considered and provides the methods required to find the optimal position to deploy the airborne relay. Chapter 6 presents the numerical results obtained by applying the methods of Chapter 5. Finally, Chapter 7 concludes the thesis.

Chapter 2

Probability of Obtaining Line-of-Sight in a Poisson Forest

Consider a pair of ground vehicles located in a planar workspace (*e.g.* a forest) with stochastically distributed obstacles (*e.g.* trees) of non-trivial thickness. The location of the obstacles can be described by a two-dimensional Poisson Point Process (PPP) with a fixed density λ_f describing the expected number of *potential obstacles* per unit area. Such a workspace is referred to as a *Poisson forest*.

Let N be the random variable describing the random number of obstacles in a workspace of area A_f in a *Poisson forest*. The probability that N equals to a specific number n of obstacles is

$$\mathbb{P}\{N = n\} = \frac{(\lambda_f A_f)^n}{n!} e^{-\lambda_f A_f}. \tag{2.1}$$

Both vehicles are equipped with communication devices at a height of h_g. The vehicles can communicate with each other using these devices if the Line-of-Sight (LoS) is not obstructed by obstacles in the environment. Only obstacles of sufficient height will block the LoS. We refer to these obstacles as *blockages*. Whether an obstacle becomes a blockage or not depends on its own height, the height of the communications devices, and where both the obstacles and the vehicles are located.

We assume the height of any obstacle is represented by a non-negative random variable H. In real-world forests, the distribution of the random variable H may vary [21–23]. Notice that we use a truncated Gaussian distribution and a uniform distribution in this thesis to illustrate our proposed method, but our analysis is not limited to any specific distribution. The truncated Gaussian distribution used in this thesis is created by taking a Gaussian random variable (with mean μ and standard deviation σ) and conditioning the variable on $h \geq 0$. Let $F_H(\cdot)$ denote the cumulative distribution function (CDF) of the random variable H. The CDF of H is as follows

$$F_H(h) = \frac{Q\left(\frac{\mu - h}{\sigma}\right) - Q\left(\frac{\mu}{\sigma}\right)}{1 - Q\left(\frac{\mu}{\sigma}\right)}, \tag{2.2}$$

for $h \geq 0$, and zero otherwise. $Q(\cdot)$ is the Q-function. This function is defined as follows

$$Q(x) = \frac{1}{\sqrt{2\pi}} \int_x^\infty \exp\left(-\frac{u^2}{2}\right) du$$

A uniform distribution assumes that the heights of the obstacles are distributed evenly across 0 to $h_{\max}$, where $h_{\max}$ is the maximum possible height of obstacles in this workspace. Let h_a be the height of the air-borne relay. In this thesis, we assume $h_g < h_{\max} < h_a$, where h_g is the height of the communication devices. The CDF of H in this case is

$$F_H(h) = \begin{cases} 0 & \text{for } h < 0 \\ \dfrac{h}{h_{\max}} & \text{for } 0 \leq h \leq h_{\max} \\ 1 & \text{for } h > h_{\max} \end{cases} \tag{2.3}$$

Consider a pair of vehicles i and j deployed on the ground, and set the ground plane as the $x - y$ plane. Let the position of ground vehicle i as the origin, and the x-axis go through the ground vehicle j. The locations of both ground vehicles are therefore $(0, 0)$ and $(g, 0)$, where g is the

Euclidean distance between them. The location of the air-borne relay's projection on the $x - y$ plane is denoted as (x_a, y_a). The planar distance between the ground vehicle i and the air-borne relay's projection is denoted as r_a, such that $r_a^2 = x_a^2 + y_a^2$.

Only obstacles along the straight line connecting $(0, 0)$ and $(g, 0)$ can potentially block the LoS between ground vehicles i and j. Similarly, only obstacles along the straight line connecting $(0, 0)$ and (x_a, y_a) can potentially become blockages obstructing the LoS between ground vehicle i and the air-borne relay.

In a Poisson forest with a fixed density λ_f, assuming the average thickness of the obstacles is $E(W)$, the number of obstacles along a unit length of a straight line is governed by a 1-dimensional Poisson Point Process (1-D PPP) with a density denoted as λ_0. The density can be calculated by $\lambda_0 = E(W)\lambda_f$. That is to say, the expected number of obstacles between the two ground vehicles is $g\lambda_0$ and the expected number of obstacles between the ground vehicle i and the air-borne relay is $r_a\lambda_0$. Among these obstacles, only those whose heights are above certain thresholds will actually become blockages of the LoS. We refer to these thresholds as *critical heights*, and denote it as h_c.

The critical height for an obstacle to blocking the LoS between a pair of ground vehicles both with communication devices at a height of h_g is constantly $h_c = h_g$ along the straight line connecting both vehicles. However, h_c does not remain a constant while considering the LoS between a ground vehicle and an air-borne relay deployed at $h_a > h_g$. Fig. 2.1 shows that h_c varies along the straight line connecting a ground vehicle and the air-borne relay. For the ground vehicle i deployed at $(0, 0)$ carrying a communication device at $(0, 0, h_g)$, and the air-borne relay deployed at a planar distance of r_a and a height of h_a, the critical height h_c is a function of the Euclidean distance between the obstacle and the ground vehicle, which is denoted as r. Therefore, $h_c(r)$ can be calculated as

$$h_c(r) = \frac{h_a - h_g}{r_a} r + h_g. \tag{2.4}$$

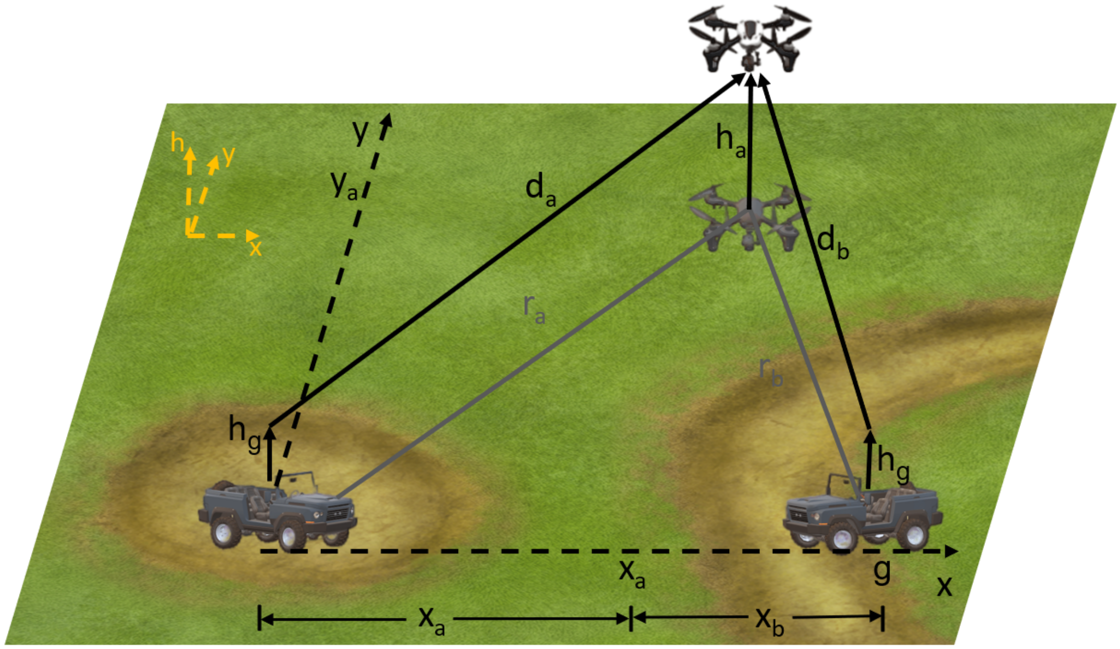

Figure 2.1: Positions of the airborne relay and ground vehicles. The ground vehicles are located at coordinates $(0, 0)$ and $(g, 0)$. Their communication devices are both at a height of h_g. The airborne relay is at a height of h_a, with (x_a, y_a) as its projection on the ground plane. r_a and r_b are the horizontal distances from the ground vehicles to the airborne relay's projection on the ground plane. d_a and d_b are the Euclidean distances between the communication devices of the ground vehicles and the airborne relay.

For any random obstacle, assuming its height is h_o, the probability that h_o is greater than a given h_c can be calculated by

$$\mathbb{P}\{h_o > h_c\} = 1 - F_H(h_c).$$

Therefore, the distribution of *blockages* (*i.e.* obstacles above a given critical height h_c) along a straight line in a Poisson forest can be modeled as a PPP with its density λ_c defined as follows

$$\lambda_c = \lambda_0 \mathbb{P}\{h_o > h_c\} = \lambda_0 \left[1 - F_H\left(h_c\right)\right]. \tag{2.5}$$

When h_c is not a constant, as in the case of the ground-air link, where h_c is distance-dependent as it is shown in Eq. (2.4), the 1-D PPP describing the location of the blockages becomes an *inhomogeneous Poisson point process*. We denote the distance-dependent density of this inhomogeneous PPP as $\lambda(r)$ and define it as

$$\lambda(r) = \lambda_0 \left[1 - F_H\left(h_c\left(r\right)\right)\right]. \tag{2.6}$$

For a given distribution $F_H(\cdot)$ of the obstacles' heights, the cumulative probability towards a given h_c increases with h_c. Therefore, $\lambda(r)$ decreases monotonically when h_c increases. In a given Poisson forest, with a greater critical height determined by the height and altitude of the vehicles for the ground-air link, the probability of having potential obstacles taller than this critical height is smaller than in the case of the ground-ground link. We then calculate the probability of preserving LoS between a pair of ground vehicles in a Poisson forest directly, as well as via the aid of an air-borne relay.

2.1 LoS Probability Between a Pair of Ground Vehicles

The critical height between a pair of ground vehicles is constant. The probability of preserving LoS between a pair of ground vehicles located at $(0, 0)$ and $(g, 0)$ can be computed from the void probability of the homogeneous PPP in Eq. (2.1) with density described by Eq. (2.5) over the interval $r = [0, g]$. The LoS probability for the ground-ground link is

$$\mathbb{P}_{LoS}^{gg}(r) = e^{-\lambda_0[1-F_H(h_g)]r}. \tag{2.7}$$

In Eq. (2.7), it is observed that the LoS probability is monotonically decreasing. It decreases as the distance between the ground vehicles increases. The explanation of this behavior is straightforward. As the distance between the ground vehicles increases, it is more likely the existence of blockages between the ground vehicles.

2.2 Ground-Air LoS Probability

The distribution of obstacles along the straight line from one ground vehicle to the airborne relay can be modeled as a PPP with the density λ_0 defined as in Eq. (2.6), where the critical height $h_c(r)$ is defined as in Eq. (2.4).

The probability of preserving the LoS between the ground vehicle and the airborne relay is found from the void probability of the inhomogeneous PPP as follows

$$\mathbb{P}_{LoS}^{ga}(r_i) = \exp\left(-\int_0^{r_i} \lambda(r)dr\right), \tag{2.8}$$

where r_i is the planar distance between the ground vehicle i and the airborne relay's ground projection. It is important to note that the LoS probability is reciprocal. The LoS probability from a ground vehicle to the airborne relay is the same as the LoS probability from the airborne relay to the same ground vehicle. Whether a closed-form expression to the solution of Eq. (2.8) can be found depends on the type of distribution $F_H(\cdot)$. When H takes the form of a uniform or truncated Gaussian distribution, the closed-form expression is relatively easy to find. If a closed-form solution is unavailable, Eq. (2.8) can still be solved via numerical methods.

2.3 A Pair of Ground Vehicles Aided by an Airborne Relay

While using an airborne relay to aid the communication between two ground vehicles i and j, the communication between the airborne relay and both ground vehicles may suffer from blockage. In this case, the LoS preservation probability is the joint probability of the LoS probability between ground vehicle i and the airborne relay, and the LoS probability between the airborne relay and the ground vehicle j. We denote the probability of having an unobstructed *air-aided* communication between the two ground vehicles as $\mathbb{P}^{gag}_{LoS}$, which can be computed as

$$\mathbb{P}^{gag}_{LoS}(r_i, r_j) = \mathbb{P}^{ga}_{LoS}(r_i)\mathbb{P}^{ga}_{LoS}(r_j), \tag{2.9}$$

where r_i is the distance from the airborne relay's ground projection to ground vehicle i (which is located at the origin of the $x - y$ plane) and r_j is the distance from the airborne relay's ground projection to ground vehicle j, which is located at $(g, 0)$. Eq (2.9) assumes that the two LoS probabilities on the right hand side are independent. This will be true if the two ground vehicles are far enough apart, which is the usual case when the air vehicle is used as a relay. However, if the ground vehicles are close or if their angle of incidence at the relay is small, the the two probabilities may be correlated [26].Due to the reciprocity in the LoS probability (*i.e.*, if the ground vehicle can see the air vehicle, then the air vehicle can see the ground vehicle)), we have that the ground-air and air-ground LoS probabilities are equal.

In this chapter, the model considered for describing the position of the obstacles and their heights were defined. With this, In Chapter 3, closed-form expression for the LoS probability between the two ground vehicles when the air vehicle is deployed are presented. Then, in addition to the LoS probability, a new metric is presented to determine the quality of the communication links.

Chapter 3

Air-Aided Communication of a Pair of Ground Vehicles

This chapter first calculates the LoS probability of a two-hop air-aided communication between a pair of ground vehicles. We assume truncated Gaussian and uniform distributions for the obstacle heights. The airborne relay is assumed to be deployed above the mid-point of the two ground vehicles. We then define and compute the *throughput* in Sec. 3.3 to evaluate the quality of the communication considering both the preservation of the communication path and the loss of signal power.

3.1 LoS Probability for Truncated Gaussian Distribution of the Obstacles' Heights

For the ground-air link, the density of the inhomogeneous PPP describing the location of the blockages along the straight line joining the positions of a ground vehicle and the airborne relay is given by Eq. (2.6). In this equation, when the distribution of the obstacles' heights is modeled by the truncated Gaussian distribution, $F_H(\cdot)$ is given by Eq. (2.2). Substituting $F_H(\cdot)$ in Eq. (2.6), the density of the inhomogeneous PPP can be expressed as

$$\lambda(r) = \lambda_0 \left(\frac{\Phi\left(\frac{\mu - h_c(r)}{\sigma}\right)}{\Phi\left(\frac{\mu}{\sigma}\right)} \right).$$

where

$$\Phi(z) = 1 - Q(z) = \frac{1}{2}\left(1 + \text{erf}\frac{z}{\sqrt{2}}\right) \tag{3.1}$$

is the CDF of the standard normal distribution. Substituting the value of $\lambda(r)$ into Eq. (2.8) gives

$$\int_0^{r_i} \lambda(r)dr = \frac{\lambda_0}{\Phi\left(\frac{\mu}{\sigma}\right)} \int_0^{r_i} \Phi\left(\frac{\mu - h_c(r)}{\sigma}\right) dr.$$

Using Eq. (3.1), the integral on the right side can be rewritten as

$$\int_0^{r_i} \lambda(r)dr = c\left(r_i + \int_0^{r_i} \text{erf}(a - br)dr\right) \tag{3.2}$$

where $a = (\mu - h_g)/(\sqrt{2}\sigma)$, $b = (h_a - h_g)(\sqrt{2}\sigma r_i)$ and $c = \lambda_0/\left(2\Phi\left(\mu/\sigma\right)\right)$.

The solution of the integral on the right side of Eq. (3.2) is not straightforward. However, the result can be found in mathematical handbooks (*e.g.* [27]) to be

$$\int_0^{r_i} \text{erf}(a - br)dr = r_i k. \tag{3.3}$$

where

$$k = \frac{e^{-a^2} + \sqrt{\pi}\left[(m-a)\text{erf}(a-m) + a\text{erf}(a)\right] - e^{-(a-m)^2}}{\sqrt{\pi}m}, \tag{3.4}$$

and $m = (h_a - h_g)(\sqrt{2}\sigma)$. With this result, the LoS probability between a ground vehicle and the airborne relay can be found by substituting Eq. (3.2) into Eq. (2.8) with the integral on the right side of Eq. (3.2) set to the result in Eq. (3.3). The result of $\mathbb{P}^{ga}_{LoS}(r_i)$ is as follows

$$\mathbb{P}^{ga}_{LoS}(r_i) = e^{-r_i(c+ck)}. \tag{3.5}$$

Eq. (3.5) allows to compute the ground-air LoS probability when the truncated Gaussian distribution is considered. The ground-air-ground LoS probability can be computed using Eq. (2.9) and evaluating Eq. (3.5) at r_a and r_b.

3.2 LoS Probability for Uniform Distribution of the Obstacles' Heights

When the distribution of the obstacles' heights is represented by the uniform distribution, the value of $F_H(\cdot)$ in the density λ_c of the inhomogeneous PPP describing the location of the blockages is given by Eq. (2.3). It can be observed that Eq. (2.3) is a piecewise function. Evaluating $F_H(h_c(r))$ and expressing the intervals of the piecewise function in terms of the distance r_i between a ground vehicle and the airborne relay gives

$$F_H(h_c(r)) = \begin{cases} 0 & \text{for } r \leq r' \\ \left(\dfrac{h_a - h_g}{r_i h_{\max}}\right) r + \dfrac{h_g}{h_{\max}} & \text{for } r' < r \leq r_c \\ 1 & \text{for } r > r_c \end{cases} \tag{3.6}$$

where $r' = h_g r_i/(h_a - h_g)$ and r_c is the critical distance. Any obstacle located at a distance $r > r_c$ is not able to block LoS. At $r > r_c$, the critical height $h_c(r)$ is greater than the maximum height of the obstacles. It is $h_c(r) > h_{\max}$. This distance is given by

$$r_c = \left(\frac{h_{\max} - h_g}{h_a - h_g} \right) r_i. \tag{3.7}$$

Let the height at which the airborne relay is deployed be greater than the height of the ground vehicles. From the definition of r', we can observe that this is a negative value. Therefore, the interval $r \leq r'$ is not considered in Eq. (3.6).

Substituting Eq. (3.6) into Eq. (2.6) without considering $r \leq r'$, the density of the inhomogeneous PPP becomes a piecewise function as follows

$$\lambda(r) = \begin{cases} \lambda_0 \left[1 - \left(\frac{h_a - h_g}{r_i h_{\max}} \right) r - \frac{h_g}{h_{\max}} \right] & \text{for } 0 < r \leq r_c \\ 0 & \text{for } r > r_c. \end{cases} \tag{3.8}$$

In Eq. (2.6), we can observe that the density of the inhomogeneous PPP describing the blockages is zero when $r > r_c$. It agrees with the definition of the critical distance. For distances greater than r_c, none of the obstacles will be able to block the LoS. Therefore, the density of the blockages is zero since there are no obstacles taller than $h_c(r)$ at those distances. In Eq. (2.8), it is required integrating $\lambda(r)$ in the interval $[0, r_i]$. The integral of $\lambda(r)$ in this interval is

$$\int_0^{r_i} \lambda(r) dr = \int_0^{r_i} \lambda_0 \left[1 - \left(\frac{h_a - h_g}{r_i h_{\max}} \right) r - \frac{h_g}{h_{\max}} \right] dr. \tag{3.9}$$

There are two possible cases for the value of r_i. $r_i \leq r_c$ and $r_i > r_c$. When $r_i > r_c$, r can take values greater than r_c, then for $r > r_c$, $\lambda(r) = 0$ and the integral from r_c to r_i is zero. In this case, the integral has the same form as in Eq. (3.9) but with the upper limit set to r_c. We can express both integration cases of $\lambda(r)$ as follows

$$\int_0^{r_i} \lambda(r)dr = \int_0^{\min(r_i,r_c)} \lambda_0 \left[1 - \left(\frac{h_a - h_g}{r_i h_{\max}}\right) r - \frac{h_g}{h_{\max}}\right] dr. \tag{3.10}$$

Depending on the height at which the airborne relay is deployed, the value of $\min(r_i, r_c)$ changes. When the airborne relay is deployed above the maximum height of the obstacles $h_{\max}$ considered by the uniform distribution, then $\min(r_i, r_c) = r_c$. When the airborne relay is deployed at a height $h_a \leq h_{\max}$, then $\min(r_i, r_c) = r_i$.

As introduced in Chapter 2, we assume the airborne relay is deployed at a height above the maximum height of the obstacles $h_{\max}$ when the uniform distribution is used for describing the obstacles' heights. Therefore we have $\min(r_i, r_c) = r_c$. Let $\Lambda_u(\cdot)$ be the solution of the integral in Eq. (3.10). It is equal to

$$\Lambda_u(r_i) = \lambda_0 r_c \left[1 - \frac{h_g}{h_{\max}} - \left(\frac{h_a - h_g}{2 r_i h_{\max}}\right) r_c\right].$$

Substituting the value of the integral in Eq. (2.8) by Λ_u, the LoS probability for the ground-air link when the uniform distribution is considered is equal to

$$\mathbb{P}_{LoS}^{ga}(r_i) = e^{-\Lambda_u(r_i)}. \tag{3.11}$$

when the ground-air-ground link is considered, the probability of having LoS simultaneously from the airborne relay to both ground vehicles a and b is given by

$$\mathbb{P}_{LoS}^{gag}(r_i, r_j) = e^{-\Lambda_u(r_i)} e^{-\Lambda_u(r_j)}. \tag{3.12}$$

3.3 Throughput of the Communication Links

Notice that the results in Sec. 3.1 and Sec. 3.2 suggest that the LoS probability will converge to 1 if the airborne relay's height increases towards infinity. While the existence of a communication path is almost guaranteed, the capacity of the link decreases and the transmission rate may not satisfy the communication requirements.

We defined a new metric, the *throughput*, to capture the loss of signal power due to the distance together with the LoS preservation. The metric strikes a balance between LoS probability and capacity [24, 25]. In this thesis, the *throughput* is defined as the maximum achievable data rate when accounting for the possibility of blockages. It describes the expected capacity of the link in the presence of blocking, where the expectation is with respect to the LoS probability. For a single hop, the throughput is

$$T = \mathbb{P}_{LoS} C. \tag{3.13}$$

where C is the *capacity* of the link. The multiplication by $\mathbb{P}_{LoS}$ accounts for the expectation being with respect to the LoS. In this thesis, we set C as the Shannon Capacity, which is the maximum achievable rate of an unblocked link. The Shannon capacity can be defined as

$$C = B \log_2 \left(1 + SNR\right), \tag{3.14}$$

where B is the signal bandwidth, and SNR is the signal-to-noise ratio. When B is in units of Hertz, C is in units of bits-per-second (bps). When expressed in decibels, the value of SNR is

$$SNR^{\mathsf{dB}} = SNR_0^{\mathsf{dB}} - 10\alpha \log_{10}\left(\frac{d}{d_0}\right), \tag{3.15}$$

where α is the path-loss exponent, d_0 is a reference distance (typically set to 1 meter), d is the transmission distance, SNR_0^{dB} is the SNR when the receiver is placed at a distance d_0 and the free-space propagation is assumed up to that distance.

The capacity in Eq. (3.14) is zero for a blocked communication link. For random blockages, the capacity of a link is a random variable that assumes a value of C with probability $\mathbb{P}_{LoS}$ and a value of zero with probability $1 - \mathbb{P}_{LoS}$. The expected throughput of this link is the expected value of this random variable.

For direct ground-ground transmission, the throughput can be calculated substituting into Eq. (3.13) the value of $\mathbb{P}_{LoS}$ given by Eq. (2.7) and the value of C given by Eq. (3.14) considering the Euclidean distance between the ground vehicles as the transmission distance.

For a two-hop communication, the throughput is the expected end-to-end capacity. Let $\mathbb{P}_{LoS}^{ga}$ and $\mathbb{P}_{LoS}^{ag}$ be the LoS probabilities of the ground-air and air-ground links, respectively. Similarly, let C_{ga} and C_{ag} be the two capacities. The expected throughput for the ground-air-ground link is

$$T = \frac{1}{2}\mathbb{P}_{LoS}^{\mathsf{ga}}\mathbb{P}_{LoS}^{\mathsf{ag}} \min(C_{\mathsf{ga}}, C_{\mathsf{ag}}). \tag{3.16}$$

We assume that the airborne relay spends half of the time receiving from one ground vehicle and the other half transmitting to the other vehicle, the $1/2$ in Eq. (3.16) accounts for the time-division duplexing (TDD) operation of the airborne relay. The minimum capacity of the two links is chosen due to the maximum achievable transmission rate will be limited by the minimum capacity.

The ground-air-ground throughput as shown in Sec. 4.3 is maximized when the airborne relay is deployed above the midpoint of the ground vehicles. In this case, the distances from the airborne relay to the two ground vehicles are equal. Then, $\mathbb{P}^{ga}_{LoS} = \mathbb{P}^{ga}_{LoS}$. Since the capacity depends only on the transmission distance, the capacity for both links is equal too. Thus, when the airborne relay is located above the midpoint of the ground vehicles the throughput can be expressed as

$$T = \frac{1}{2}\left(\mathbb{P}^{\mathsf{ga}}_{LoS} C_{\mathsf{ga}}\right)^2 . \tag{3.17}$$

In Eq. (3.16) and Eq. (3.17), each capacity is found considering the Euclidean distance d between the communication devices of the vehicles. For the airborne relay, it is assumed that the 3-D location of the communication device is $(g/2, 0, h_a)$. For the ground vehicles, the location of the communication devices is assumed to be $(0, 0, h_g)$ and $(g, 0, h_g)$.

3.4 Simulation-Validated Results

We consider a Poisson forest with $\lambda_0 = 0.02$. For the obstacles' heights distribution, we considered both a truncated Gaussian distribution and a uniform distribution. The CDF $F_H(\cdot)$ of the truncated Gaussian distribution is as Eq. (2.2) with $\mu = 19$ m and $\sigma = 10$ m. For the uniform distribution, the CDF is as Eq. (2.3) with $h_{\max} = 29$ m. The choice of the parameters is consistent with the parameters in [16].

3.4.1 LoS Probability

We use Monte Carlo simulations to validate the results. Each data point in the following results is generated from $500,000$ trials. In every trial, a Poisson Forest is created. Ground vehicles and air-borne relays are placed to determine whether a LoS exists.

Fig. 3.1 shows the probability of preserving LoS between a ground vehicle and an airborne relay,

$\mathbb{P}^{ga}_{LoS}(r_a)$, with the horizontal distance r_a. In this figure, only the truncated Gaussian distribution is considered. The results for the uniform distribution are similar. The airborne relay flies at different fixed heights of 50 m, 100 m, and 200 m. The ground vehicle has a communication device fixed at the height of $h_g = 2$ m.

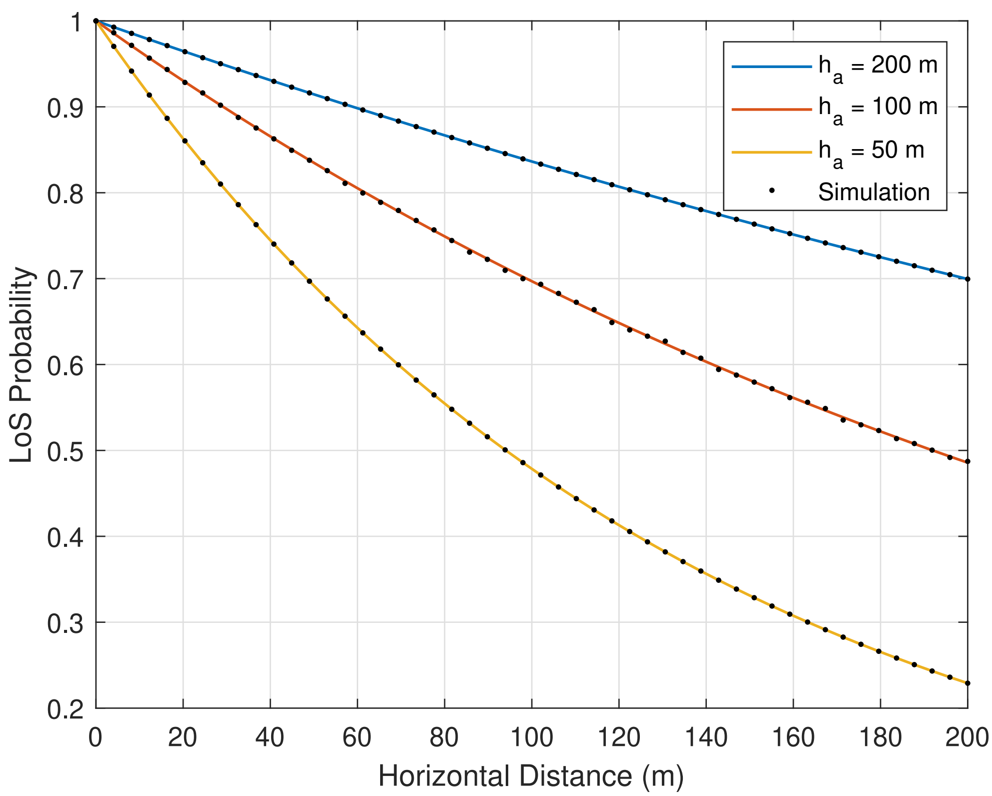

Figure 3.1: LoS probabilities for ground-ground and ground-air-ground communication. Solid lines show the numerical results calculated using our closed-form expressions, while the dots show results generated by Monte Carlo simulation. LoS probability between a ground vehicle and the airborne relay considering truncated Gaussian distribution.

The results in Fig. 3.1 show that $\mathbb{P}^{ga}_{LoS}(r_a)$ decreases as r_a increases. A longer distance between the two vehicles is expected to allow a greater probability of having blockages in between. Meanwhile, $\mathbb{P}^{ga}_{LoS}(r_a)$ increases as h_a increases. This is because the critical height will increase with a greater h_a (as it is shown in Eq. (2.4)). A greater critical height rejects more obstacles from potentially blocking the LoS between the two vehicles. Therefore, flying the airborne relay at a higher altitude generally increases the probability of obtaining LoS. Increasing the height h_g of the communication devices carried by the ground vehicles will improve the probability of obtaining LoS as well. However, it is more expensive and less efficient than increasing the height of the airborne relay.

We then compare the end-to-end LoS probability $\mathbb{P}_{LoS}$ of direct ground-ground communication with air-aided ground communication with the airborne relay always above the midpoint of the two ground vehicles, *i.e.*, $r_a = r_b = g/2$. In this scenario, the probability of obtaining LoS from the airborne relay to both ground vehicles synchronously is the square of $\mathbb{P}^{ga}_{LoS}$. We assume that the airborne relay is flying at a height of $h_a = 100$ m, while all ground vehicles have their communication devices fixed at a height of $h_g = 2$ m. Both the truncated Gaussian and the uniform height distributions are considered. Fig. 3.2 shows the results of this comparison. For direct ground-ground communication, the probability of obtaining LoS decreases much faster as a function of distance than in the case of air-aided ground communication. For the truncated Gaussian distribution, when μ = 19 m and σ = 10 m, Eq. (2.2) suggests that most of the obstacles will be taller than 2 m. Thus, almost all obstacles can block the unobstructed view between a pair of ground vehicles, severely decreasing the probability of obtaining the LoS. For the uniform distribution, according to Eq. (2.3), there is a probability greater than 0.92 that the heights of the obstacles are taller than h_g. This causes a fast decrease in the LoS probability for ground-ground communication, which is similar to what is observed for the truncated Gaussian distribution.

When $r_a = r_b = 60$ m, (*i.e.* $g = 120$ m), the probability of preserving LoS between ground vehicles using direct ground-ground communication is approximately 0.1 for both the truncated Gaussian and the uniform distributions. However, when an airborne relay is used, the probability that it preserves LoS with both ground vehicles is approximately 6.5 and 7.3 times greater than the probability of the two ground vehicles obtaining LoS over a direct link considering the truncated Gaussian and uniform distributions, respectively.

Fig. 3.2 shows that the choice of distribution does not have a significant impact on the probability of obtaining the LoS between ground vehicles using the direct link, since the communication devices of the ground vehicles are fixed at a relatively low height and therefore the LoS would be easily blocked by most obstacles. On the other hand, when an airborne relay is used, the height distribution has a bigger impact on the LoS probability since the differences in the distributions become more pronounced.

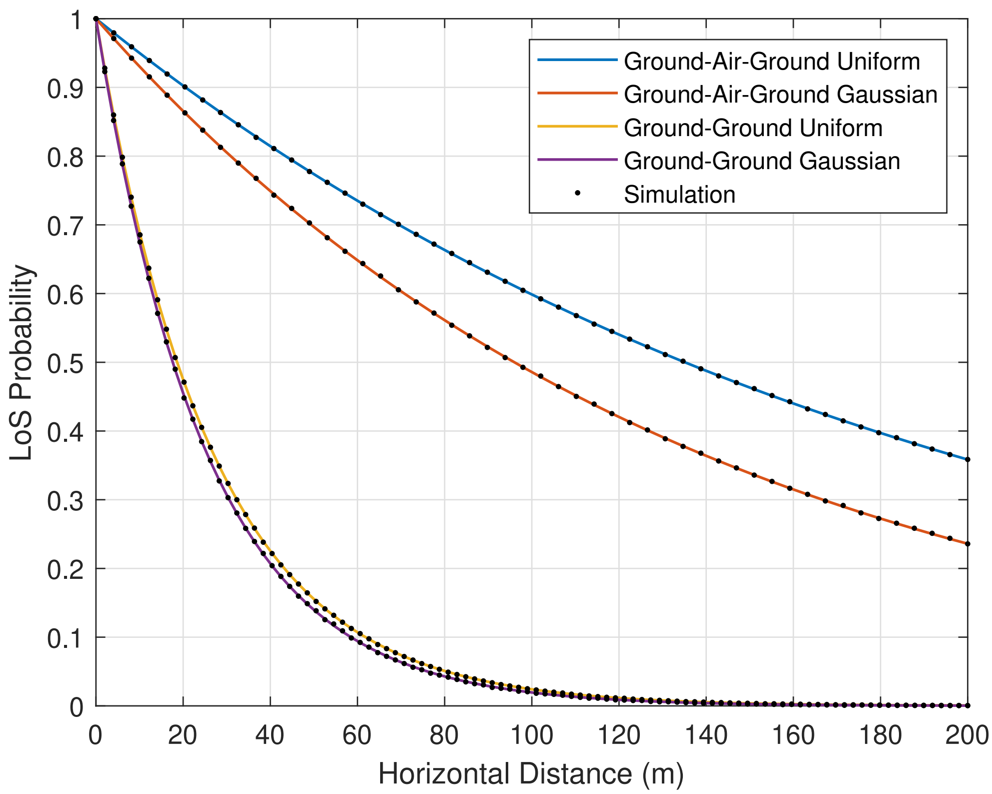

Figure 3.2: LoS probabilities for ground-ground and ground-air-ground communication. Solid lines show the numerical results calculated using our closed-form expressions, while the dots show results generated by Monte Carlo simulation. Comparison between the different cases of communication.

3.4.2 Throughput

We computed the throughput performance for the same scenarios with additional parameters set as a reference SNR of $SNR_0^{\text{dB}} = 51.98$ dB at a reference distance of $d_0 = 1$ m, a path-loss coefficient of $\alpha = 2.3$, and a bandwidth of $B = 20$ MHz. The path-loss coefficient corresponds to the one reported in [28] for the measured LoS path-loss at 38 GHz. The reference SNR is computed for a transmit power of 0 dBm, a receiver noise figure of 9 dB, and antenna gains of 12.1 dBi for both the transmit and receive antennas, which are the gains reported for a compact 6-element array operating at 38 GHz in [29]. We consider the same obstacles model as before, with $\lambda = 0.02$ and height distributions that are either a truncated Gaussian (with $\mu = 19$ m and $\sigma = 10$ m) or a uniform (with $h_{\max} = 29$ m). The ground vehicle's antenna height is set to $h_g = 2$ m.

Fig. 3.3 shows throughput as a function of the height of the airborne relay, h_a, for several different distances g between the ground vehicles. The airborne relay is located above the midpoint between the two ground vehicles, *i.e.* $r_a = g/2$, and this figure shows results for just the truncated Gaussian height distribution (results for the uniform distribution are similar). As expected, the throughput is higher when the ground vehicles are closer to each other. However, for each curve, a peak value can be observed. Lowering the altitude of the airborne relay below this peak makes it prone to blocking, but raising it above the peak value causes a loss in signal power which translates to a loss of capacity. The peak value balances the vehicles' capability of obtaining LoS and the signal power, which is a key trade-off as both contribute to the throughput. For g equal to 50 m, 100 m, and 200 m, the peak values are 100.6 Mbps, 82.7 Mbps, and 65.5 Mbps, respectively, and these peaks occur at h_a of 77 m, 134 m, and 230 m, respectively.

Fig. 3.4 shows throughput as a function of the horizontal distance g between the ground vehicles. The figure shows results for both truncated Gaussian and uniform height distributions and both direct ground-ground communication and relayed ground-air-ground communication. For ground-air-ground communication, the throughput is optimized at each distance by maximizing its value over the height of the airborne relay h_a. For direct ground-ground communication, no such optimization is possible. The plot shows that, for sufficiently far distances, the throughput of the ground-air-ground communication is higher than that of the direct ground-ground communication.

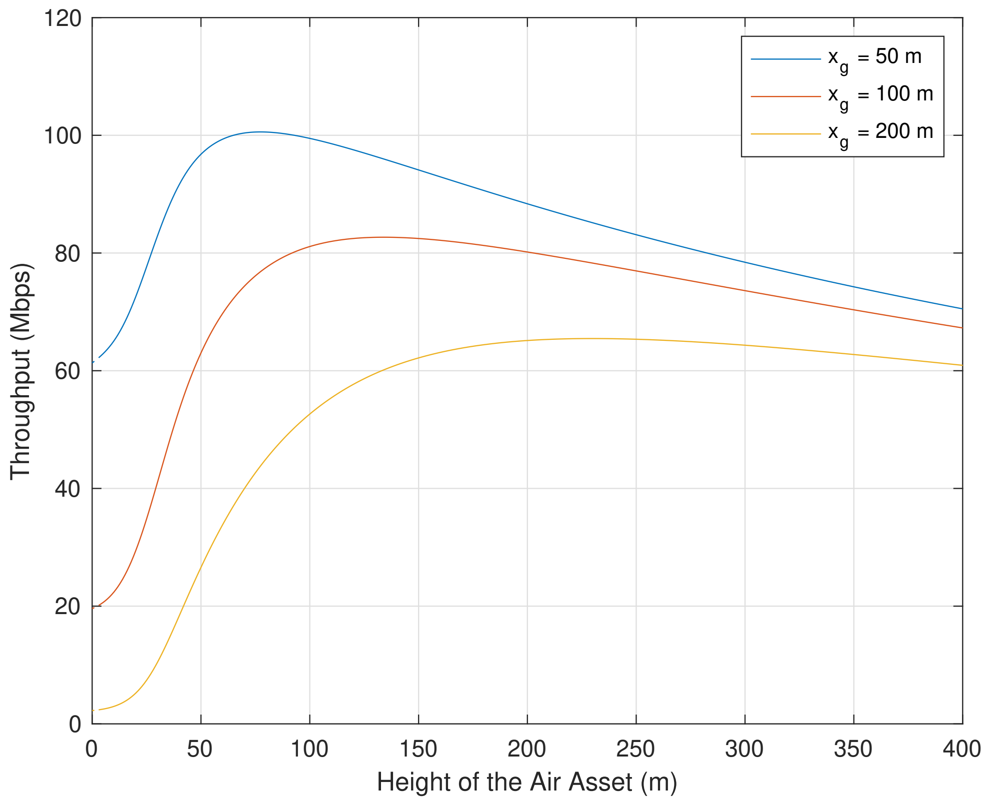

Figure 3.3: Throughput of ground-air-ground communication as a function of the height h_a of the airborne relay for different horizontal distances g. Truncated Gaussian distribution is considered. Results are shown for direct ground-ground communication as well as for relayed ground-air-ground communication. In the case of ground-air-ground communication, the throughput is optimized with respect to the height h_a of the airborne relay.

However, for shorter distances, ground-ground communication has a higher throughput. When the height distribution is a truncated Gaussian, this crossover occurs at a distance of $g = 52.9$ m, where the throughput for both direct ground-ground and relayed ground-air-ground communications is 99 Mbps. The reason that direct ground-ground communication performs better at ranges closer than this crossover distance is primarily due to the need for the airborne relay to duplex the signal received from the first ground vehicle and transmitted to the second ground vehicle. The direct link does not need to duplex. However, at longer distances, maintaining a direct link between the two ground vehicles suffers from a lower probability of obtaining a LoS and a weaker signal power due to the long single transmission path.

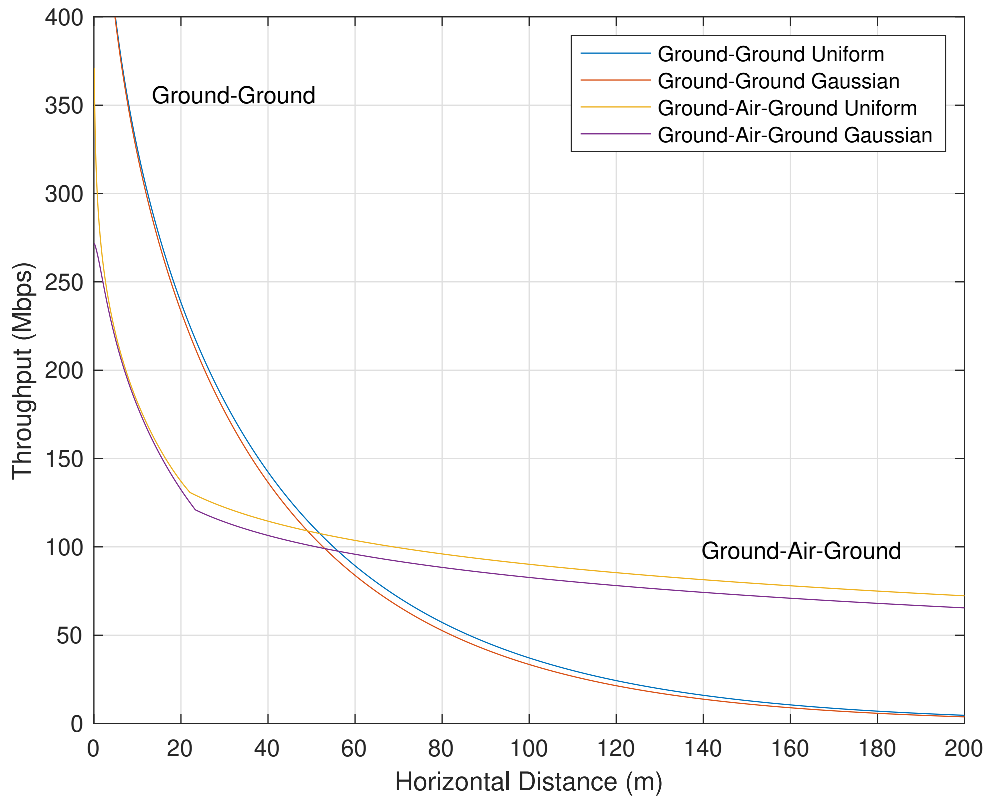

Figure 3.4: Throughput as a function of horizontal distance g for both truncated Gaussian and uniform height distributions. Results are shown for direct ground-ground communication as well as for relayed ground-air-ground communication. In the case of ground-air-ground communication, the throughput is optimized with respect to the height h_a of the airborne relay.

Chapter 4

Feasible Locations for the Airborne Relay

Chapter 3 assumed that the airborne relay is always above the mid-point of the ground vehicles, with only its height varying. In this section, we analyze the communication performance for the airborne relay deployed at different locations and determine the 3-D deployment of the airborne relay to realize the desired LoS probability and throughput.

4.1 Fixed LoS Probability

When the value of $\mathbb{P}^{ga}_{LoS}(r_i)$ is provided as a constant within the interval $(0, 1]$, Eq. (2.8) can be solved and lead to the desired horizontal distance between the ground vehicle i and the airborne relay. That is to say, the airborne relay flies above the perimeter of a circle with radius r_i and its center at where the ground vehicle i is located will always have the given probability preserving LoS with vehicle i.

For air-aided communication between two ground vehicles, it is also possible to fix the LoS probability as in Eq. (2.9) and calculate the desired locations of the airborne relay. We will demonstrate the calculation considering both the truncated Gaussian distribution and the uniform distribution for the obstacles' heights.

4.1.1 Truncated Gaussian Distribution

When H is described by a truncated Gaussian distribution as Eq. (2.2), it follows from Eq. (2.9) that the two-hop LoS probability is equal to

$$\mathbb{P}_{LoS}^{gag}(r_a, r_b) = e^{-(r_a+r_b)(c+ck)},$$

where $i = a$ and $j = b$. Fixing the desired value of $\mathbb{P}_{LoS}^{gag} = P$ gives

$$P = e^{-(r_a+r_b)(c+ck)}.$$

Rewriting this equation gives

$$r_a + r_b = c_t, \tag{4.1}$$

where $c_t = -\ln(P)/(c + ck)$. For fixed altitudes Eq. (4.1) describes an ellipse since the sum of the distances from the airborne relay to the ground vehicles a and b is constant and equal to c_t. In Fig. 2.1, it is observed that r_a and r_b can be expressed in terms of the position (x_a, y_a) of the airborne relay in the ground plane. When r_a and r_b are expressed in terms of (x_a, y_a) it is obtained

$$\sqrt{x_a^2 + y_a^2} + \sqrt{(g - x_a)^2 + y_a^2} = c_t. \tag{4.2}$$

Let $(x, y) = (x_a, y_a)$ then, Eq. (4.2) can be expressed as follows

$$\frac{4}{c_t^2}\left(x - \frac{g}{2}\right)^2 + \frac{4}{c_t^2 - g^2}y^2 = 1. \tag{4.3}$$

When the airborne relay flies above the coordinate (x, y) at a fixed altitude, it will produce the desired two-hop LoS probability P. When $g < c_t$, the positions (x, y) allowed by Eq. (4.3) form an ellipse for every h_a. This ellipse has its major axis along the x-axis (straight line joining the position of the ground vehicles) and foci located at $(0, 0)$ and $(g, 0)$ which corresponds to the positions of the ground vehicles.

4.1.2 Uniform Distribution

When H is uniform over the interval $[0, h_{\max}]$ as it shown in Eq. (2.3), the two-hop LoS probability is given by $\mathbb{P}_{LoS}^{gag}(r_i, r_j) = e^{-\Lambda_u(r_i)}e^{-\Lambda_u(r_j)}$ according to Eq. (3.12). When the airborne relay is deployed at $h_a > h_{\max}$, $\Lambda_u(\cdot)$ is equal to

$$\Lambda_u(r_i) = \lambda_0 r_{ci} \left[1 - \frac{h_g}{h_{\max}} - \left(\frac{h_a - h_g}{2r_i h_{\max}}\right) r_{ci}\right],$$

where r_{ci}, for $i \in \{a, b\}$, is the critical distance beyond which the critical height is taller than the maximum height $h_{\max}$. This distance is given by Eq. (3.7). Let $P \in [0, 1]$ be a constant value of LoS probability. Fixing the value of $\mathbb{P}_{LoS}^{gag}(r_a, r_b) = P$ with $i = a$ and $j = b$, and rewriting Eq. (3.12), the following equation is obtained

$$r_a + r_b = c_u, \tag{4.4}$$

where c_u is determined by the probability distribution of H (in this case uniform distribution), the desired value of P, the height of the ground vehicles, and the height at which the airborne relay is deployed. The value of c_u is found to be

$$c_u = \frac{-(h_a - h_g)\ln(P)}{\lambda_0(h_{\max} - h_g)\left(1 - \frac{h_g}{h_{\max}} - \frac{h_{\max} - h_g}{2h_{\max}}\right)}.$$

Similar to Eq. (4.1), for a fixed altitude of the airborne relay, Eq. (4.4) describes an ellipse, only now the two distances sum to a different value; *i.e.*, they sum to c_u. In Eq. (4.4), by expressing r_a and r_b in terms of the position of the airborne relay (x_a, y_a), the relation between the position of the airborne relay and the desired value of P can be found as follows

$$\sqrt{x_a^2 + y_a^2} + \sqrt{(g - x_a)^2 + y_a^2} = c_u. \tag{4.5}$$

After simplifying Eq. (4.5) and substituting $(x, y) = (x_a, y_a)$, it is obtained

$$\frac{4}{c_u^2}\left(x - \frac{g}{2}\right)^2 + \frac{4}{c_u^2 - g^2} y^2 = 1, \tag{4.6}$$

As with the truncated Gaussian distribution, an airborne relay flying above a coordinate (x, y) satisfying Eq. (4.6) will provide the desired two-hop LoS probability P. For a fixed h_a and $g < c_u$, the locus of all (x, y) forms an ellipse. This ellipse changes its size as the altitude of the airborne relay changes.

4.2 Fixed Link Capacity and Throughput

Sec. 4.1 found the positions of the airborne relay for a given two-hop LoS probability. Here we compute the positioning of the airborne relay for a given link capacity and a given throughput.

4.2.1 Constant Link Capacity

Using the square of the Euclidean distance $d_i^2 = x_i^2 + y_i^2 + h_a^2$ between the airborne relay and a ground vehicle i and rearranging Eq. (3.14), the following relation is found:

$$x_i^2 + y_i^2 + h_a^2 = d_0^2 \left(\frac{10^{\mathrm{SNR}_0^{\mathrm{dB}}/10}}{2^{C_i/B} - 1}\right)^{2/\alpha}. \tag{4.7}$$

When Eq. (4.7) is used to determine the positions producing constant capacity for a single hop, this equation shows that the airborne relay should be located on a circle around the ground vehicle (for fixed h_a). However, when the ground-air-ground link is considered, the end-to-end capacity is determined by the minimum capacity value of the two hops. It is $C = \min(C_a, C_b)/2$, where the multiplication by 1/2 accounts for the time-division duplexing operation at the airborne relay.

Using Eq. (4.7), it can be found the regions in the space in which the capacity is determined by the capacity of the link between the airborne relay and vehicle a or by the link between the airborne relay and vehicle b (C_a or C_b). When $d_a > d_b$ then $C_a < C_b$ and for $d_a \leq d_b$ then $C_b \leq C_a$. Solving the inequality $d_a \leq d_b$ the conditions for having the value of $\min(C_a, C_b)$ depending on the position of the airborne relay can be determined. Thus, $d_a \leq d_b$ for $x \leq g/2$. Therefore, the capacity for the ground-air-ground link is given by

$$C = \min(C_a, C_b)/2 = \begin{cases} C_b/2 & \text{if } x \leq g/2 \\ C_a/2 & \text{if } x > g/2 \end{cases}. \tag{4.8}$$

4.2.2 Constant Throughput

For a two-hop communication, the throughput is the expectation of the end-to-end capacity, where the expectation is with respect to the two-hop LoS probability; *i.e.*, it is as follows:

$$T = \begin{cases} \mathbb{P}_{LoS}^{gag} C_b/2 & \text{if } x \leq g/2 \\ \mathbb{P}_{LoS}^{gag} C_a/2 & \text{if } x > g/2 \end{cases}. \tag{4.9}$$

Fixing the value of throughput in Eq. (4.9) and allowing the 3-D position (x, y, h_a) of the airborne relay to vary, we can find a surface in 3-D space that guarantees the desired throughput. Also, the positions of the airborne relay that maximize the throughput can be found, for instance, by fixing the coordinate on the ground plane (x, y) and determining the altitude h_a that maximizes the throughput.

4.3 Numerical Illustration of the Results

We choose varying values as the given LoS probability, capacity, and throughput and demonstrate the 2-D and 3-D manifolds to deploy the airborne relay to achieve the given values. The results provide an insight into possible flight paths for the airborne relay that provide the necessary performance metrics.

Unless otherwise specified, it is assumed that the values of the key physical parameters are assumed to be $\lambda_0 = 0.02$, $h_g = 2$ m, $B = 100$ MHz, $d_0 = 1$ m, $SNR_0^{\text{dB}} = 50$ dB, and $\alpha = 2.3$. This path-loss coefficient corresponds to measured LoS path-loss at 38 GHz [28]. The value of SNR_0^{dB} corresponds to a carrier frequency of 38 GHz, a bandwidth of 100 MHz, a transmit power of 0 dBm, a receiver noise figure of 11 dB, and antenna gains of 12.1 dBi for both the transmit and receive antennas, which are the gains reported for a compact 6-element array operating at 38 GHz in [29]. Both kinds of obstacle height distributions are considered; for the case that the heights are uniform we use $h_{\max} = 29$ m and for the case that they are truncated Gaussian we use $\mu = 19$ m and $\sigma = 10$ m.

4.3.1 LoS Probability

This section shows the results obtained when the desired LoS probability P and the distance between ground vehicles g take different values in Eq. (4.3) and Eq. (4.6). Fig. 4.1 and Fig. 4.2 consider the case that $h_a = 100$ m and $g = 60$ m. In these figures, red dots indicate the positions of the two ground vehicles, while the black ellipses show the positions for the airborne relay that provide constant LoS probabilities equal to $P = 0.8$ (inner ellipse), $P = 0.65$ (middle ellipse), and $P = 0.5$ (outer ellipse). Fig. 4.1 corresponds to the case that the obstacle's height distribution is truncated Gaussian while Fig. 4.2 corresponds to the case that it is uniform. For greater LoS probability the eccentricity of the ellipses increases and for smaller probabilities, the eccentricity decreases and the major axis of the ellipse increases its length.

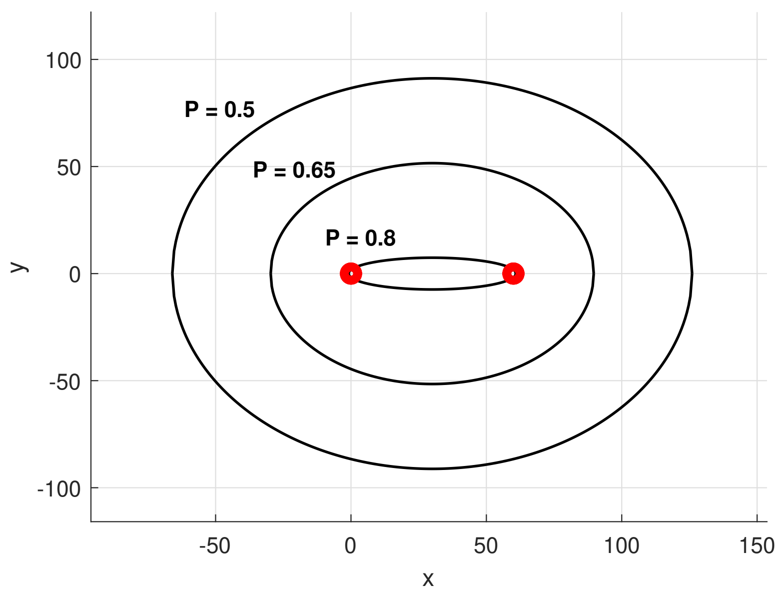

Figure 4.1: Airborne relay's positions producing fixed LoS Probability. Truncated Gaussian distribution of the obstacle's heights is considered. Red dots indicate the positions of the ground vehicles.

When h_a changes and the same LoS probability is required, the elliptic cone presented in Fig. 4.3 is obtained. This surface represents the positions that produce the desired LoS probability P. In this case, $P = 0.7$, and the uniform obstacle's height distribution is considered. The minimum height at which the airborne relay can be deployed to produce the desired P with a given distance g between ground vehicles can be determined by equating c_u to g and solving for h_a. This minimum height determines the height at which is the bottom of the elliptic cone. At the bottom of the cone $h_a = 44.29$ m.

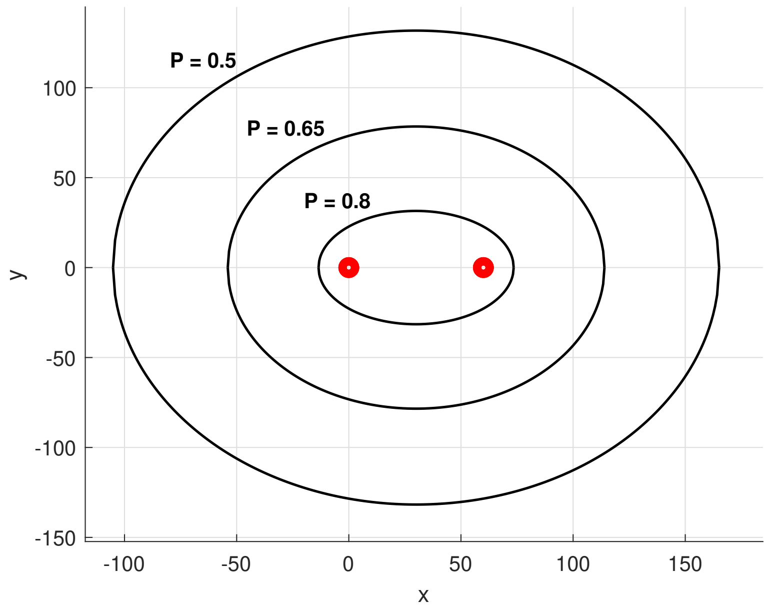

Figure 4.2: Airborne relay's positions producing fixed LoS Probability. Uniform distribution of the obstacle's heights is considered. Red dots indicate the positions of the ground vehicles.

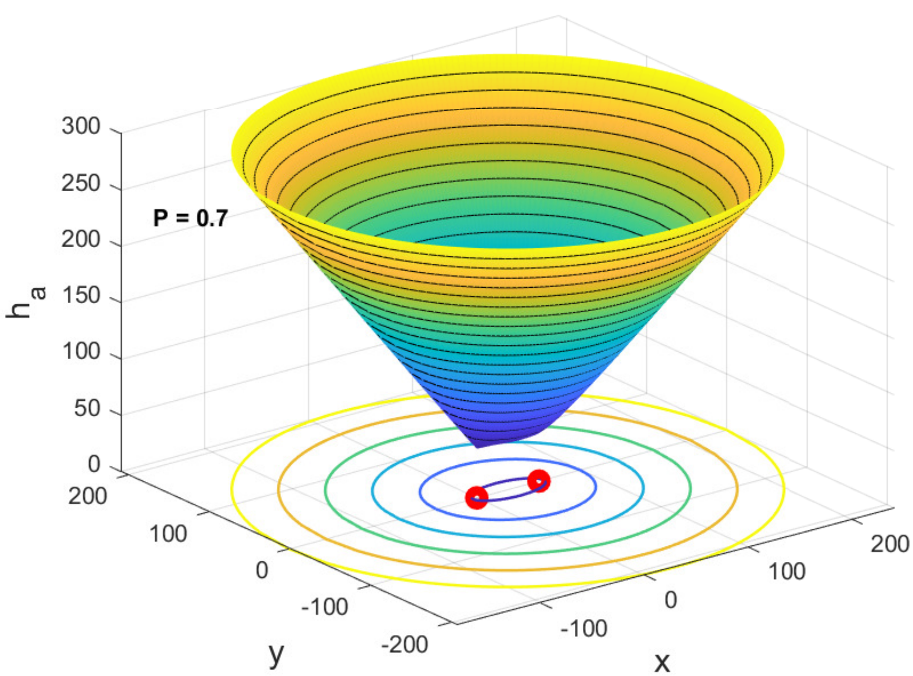

Figure 4.3: Airborne relay's positions producing $P = 0.7$. The contour plot of the surface is shown in the $x - y$ plane. Red dots indicate the positions of the ground vehicles. Uniform height distribution is considered.

4.3.2 Capacity and Throughput

In Fig. 4.4, the value of capacity in Eq. (4.8) is fixed at $C = 100$ Mbps, and the 3-D region of constant capacity is shown. When the airborne relay's position is such that $x \leq g/2$, the capacity of the ground-air-ground link is limited by the capacity of the link between the airborne relay and ground vehicle b, and the surface is obtained evaluating Eq. (4.7) at r_b. Similarly, for $x > g/2$, the capacity is determined by the link between ground vehicle a and the airborne relay, and the surface is obtained evaluating Eq. (4.7) at r_a. Any position inside the volume covered by this surface will produce a capacity greater than 100 Mbps. Because capacity does not account for the presence of obstacles, the region does not depend on the obstacle height distribution.

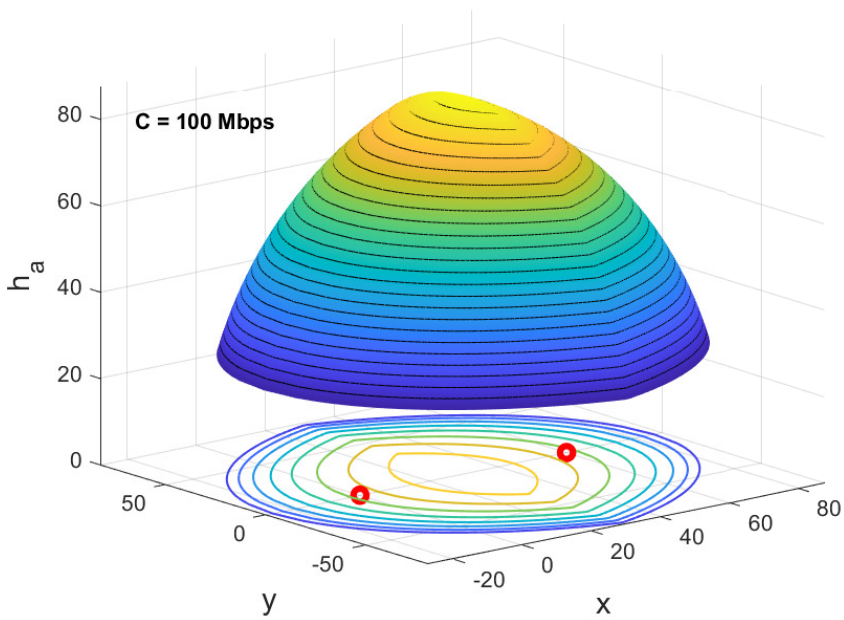

Figure 4.4: Airborne relay's positions producing $C = 100$ Mbps. The contour plot of the surface is shown in the $x - y$ plane. Red dots indicate the positions of the ground vehicles. Uniform height distribution is considered.

Next, we consider regions of constant throughput, as it is a metric that balances capacity with LoS probability. Fig. 4.5 shows a 3-D surface representing the positions of the airborne relay that guarantee a throughput equal to 80 Mbps when the uniform height distribution is considered. The following observations can be made about the surface that is shown. As shown in Fig. 4.3, it can be observed that as the height h_a of the airborne relay increases, the contours of constant line-of-sight (LoS) probability expand, indicating a larger area covered by LoS connections. On the other hand, in Fig. 4.4, as the height h_a increases, the contours of constant capacity shrink. These observations highlight the contrasting effects of airborne relay's height on LoS probability and capacity. Since the throughput is the product of LoS probability and capacity, in Fig. 4.5, both behaviors are observed, with the cross-section areas initially increasing with h_a as the regions of constant LoS probability expand. But then, after a certain height of $h_a \geq 53.6$ m, the area of the cross sections decreases as the constant-capacity contours contract with increasing h_a. The volume of the region contained by the surface is inversely proportional to the throughput; *i.e.*, if a smaller throughput were considered, then the region shown would be larger.

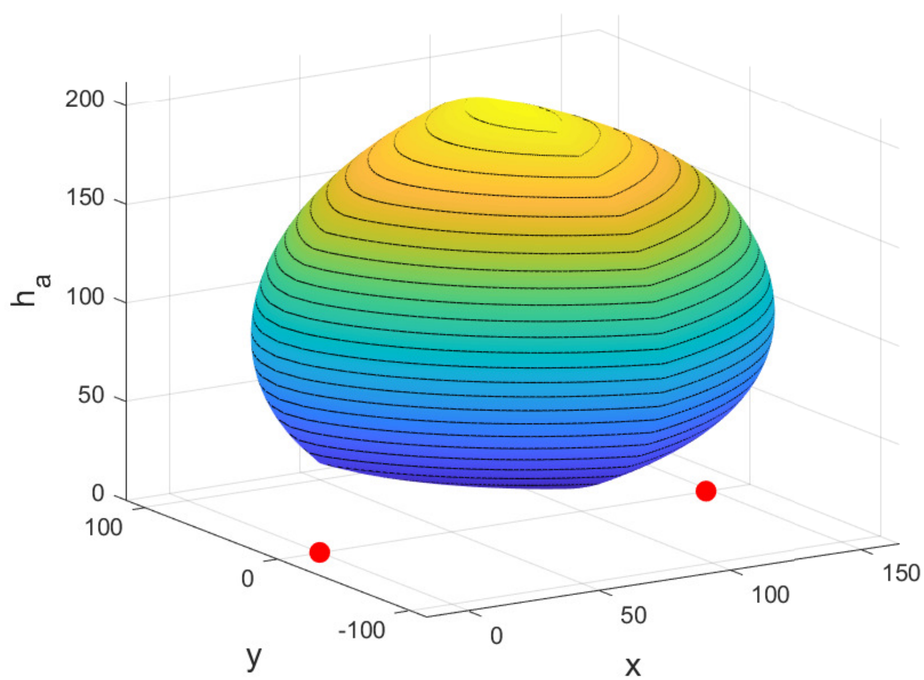

Figure 4.5: Airborne relay's positions producing $T = 80$ Mbps. The obstacle heights are uniformly distributed.

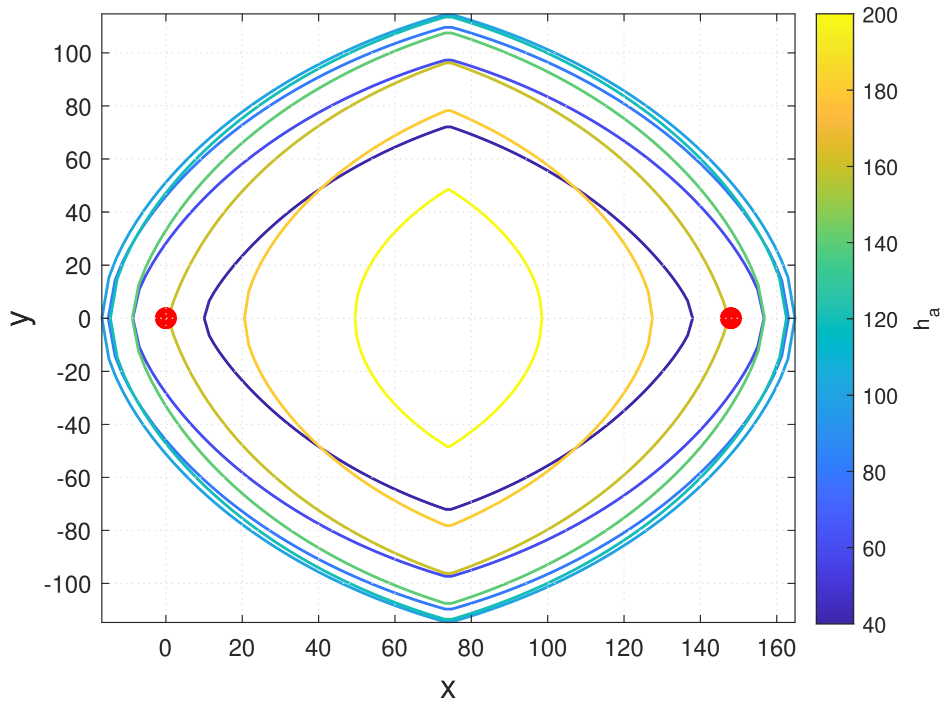

Figure 4.6: Contour plot of the surface is shown in Fig. 4.5.

In addition to identifying regions of constant throughput, it is also possible to optimize equation Eq. (4.9) with respect to the height h_a of the airborne relay. This optimization process determines the airborne relay height that maximizes the throughput for a given position in the ground plane. Fig. 4.7 shows the airborne relay's heights that maximize throughput for each position of the airborne relay over the ground plane. It is observed that the maximum possible throughput is obtained when the airborne relay is located in $(g/2, 0, 36.3)$ for $g = 60$ m. The surface shown in Fig. 4.7 allows us to determine the positions across which the airborne relay should move if it is required to obtain the maximum possible throughput for any of the positions. Additionally, the contours for different heights of the surface in Fig. 4.7 are shown in the $x - y$ plane.

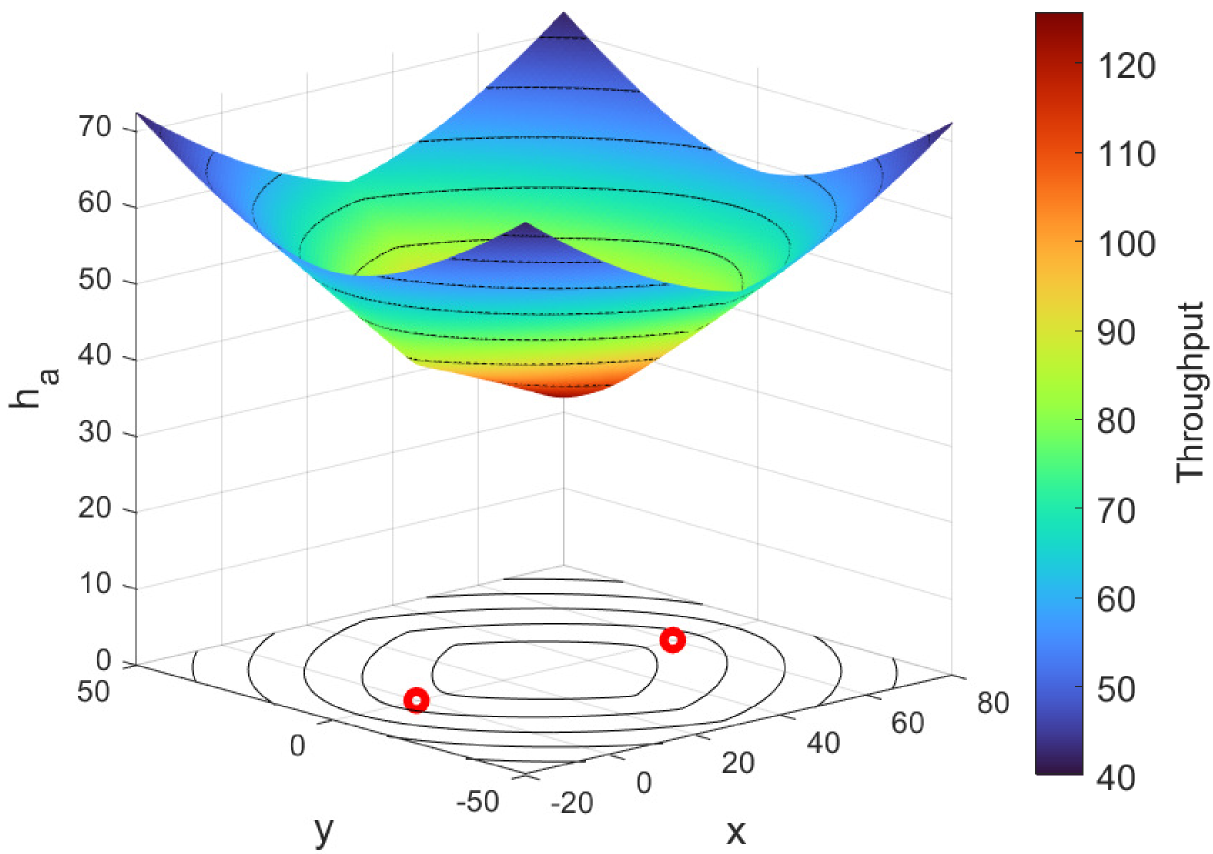

Figure 4.7: Height of the airborne relay maximizing the throughput for each position onto the ground plane. The color of the surface represents the value of throughput indicated by the color bar. The contours in the $x - y$ plane represent the contours for the same airborne relay's height. The obstacle's heights are uniformly distributed.

Chapter 5

Airborne Relay for Multiple Ground Vehicles

In this chapter, we provide methods to calculate the optimized 3-D positions for an airborne relay to maximize the air-aided communication performance in a network of multiple ground vehicles.

5.1 Communication Graph of Multiple Ground Vehicles

To find the optimal position to deploy the airborne relay when $N \geq 2$ ground vehicles are considered, we first model the communication network of multiple ground vehicles as a graph $\mathcal{G} = (\mathcal{V}, \mathcal{E})$, where each node v_i in the vertice set $\mathcal{V}$ represents a ground vehicle, and each edge $e_{i,j}$ in the edge set $\mathcal{E}$ refers to the communication link between a pair of ground vehicles i and j. Each edge has a weight that represents the best-expected throughput it can achieve. For a pair of ground vehicles that can communicate both directly and via the airborne relay, the weight reflects the better throughput achieved by the two different communication means. The communication between vehicles is assumed to be bidirectional (agents can receive and send information using the same link), therefore the edges in the graph $\mathcal{G}$ are undirected.

Assuming that all nodes in the communication network are equivalently important, there are two aspects of a communication graph that we care about. The first is the expected throughput of all communication links. Here we define a notation $T_{\mathcal{G}}$ such that

$$\frac{1}{T_{\mathcal{G}}} = \frac{1}{N(N-1)/2} \cdot \sum_{v_i, v_j \in \mathcal{V}} \frac{1}{T_{ij}}. \tag{5.1}$$

Such that the expected time of delivering information packages over a link with the expected throughput $T_{\mathcal{G}}$ is the average time of delivering the same packages over any of the links in the communication graph.

The second aspect is whether the throughput is evenly distributed across all links in the network. We borrow concepts from spectral graph theory [30] to analyze the *layout* of this communication network modeled as graph $\mathcal{G}$. We create the Laplacian matrix $L(\mathcal{G})$ of graph $\mathcal{G}$ as follows

$$[L(\mathcal{G})]_{ij} = \begin{cases} \dfrac{-T_{ij}}{\sqrt{T_i T_j}} & \text{for } i \neq j \\ \\ 1 & \text{for } i = j \end{cases}, \tag{5.2}$$

for $i, j = 1, \ldots, N$, where T_{ij} is the weight of the edge between the vertices i and j, and T_i defined as

$$T_i = \sum_{i \neq k, v_k \in \mathcal{V}} T_{ik}.$$

T_{ij} is chosen by $T_{ij} = \max(T_{ij}^{gg}, T_{ij}^{gag})$ and is the throughput of the link with the better quality (from the direct link or the ground-air-ground link) between the vehicles i and j. Notice that whether the direct link or the air-aided link yields a better quality for a communication link depends on the position of the airborne relay.

We denote the *second smallest* eigenvalue of $L(\mathcal{G})$ as $\lambda_2(\mathcal{G})$. This is an indicator broadly used to estimate the *connectivity* of a graph [30,31]. For a graph of $N \geq 2$ nodes with *all links* assumed to have a positive weight, and the Graph Laplacian created following Eq. (5.2), $\lambda_2(\mathcal{G})$ is bounded by

$0 < \lambda_2(\mathcal{G}) \leq \frac{N}{N-1}$. The first inequality is guaranteed if $\mathcal{G}$ remains a connected graph [30], which is established as long as all throughputs are strictly positive. A greater $\lambda_2(\mathcal{G})$ indicates a more evenly distributed throughput across all communication links. $\lambda_2(\mathcal{G})$ reaches its upper bound $\frac{N}{N-1}$ when all links enjoy the same expected throughput.

In practice, we prefer a communication network that has its aspects, the overall throughput $T_{\mathcal{G}}$, and the connectivity indicator $\lambda_2(\mathcal{G})$, both improved by adding an airborne relay. We denote the evaluating metric of the communication network as $\mathcal{Q}_{\mathcal{G}}$. Depending on the requirements of the task, the evaluation metric can be chosen in various ways, such as $T_{\mathcal{G}}^a \lambda_2(\mathcal{G})^b$, or $aT_{\mathcal{G}} + b\lambda_2(\mathcal{G})$ with a and b both positive weighting factors defined by the task requirements. In the following analysis, we demonstrate our calculation based on the metric chosen as $\mathcal{Q}_{\mathcal{G}} = T_{\mathcal{G}} \lambda_2(\mathcal{G})$.

When N $= 2$ (only two ground vehicles are considered), $\lambda_2(\mathcal{G})$ is equal to 2, and $T_{\mathcal{G}}$ is the maximum throughput between the direct link or the ground-air-ground link of the ground vehicles

$$\mathcal{Q}_{\mathcal{G}} = 2 \max(T_{12}^{gg}, T_{12}^{gag}). \tag{5.3}$$

For $N \geq 3$, analytical expressions for $\lambda_2(\mathcal{G})$ and $\mathcal{Q}_{\mathcal{G}}$ become lengthy but are still able to obtain.

5.2 Optimal Position of the Airborne Relay

This section presents the algorithm used to find the optimal position of the airborne relay producing the greatest value of $\mathcal{Q}_{\mathcal{G}}$. Algorithm 1 shows the search algorithm designed to find such a position. This algorithm computes the value of $\mathcal{Q}_{\mathcal{G}}$ produced by the positions of the airborne relay inside a predefined search region in the 3-D space. Then, finds the position producing the highest $\mathcal{Q}_{\mathcal{G}}$. To compute the throughput of each link (direct link or air-aided link) it is assumed that multiple pairs of ground vehicles can use the airborne relay at the same time without having limitations on the throughput that each air-aided link requires (*i.e.* the number of pairs of ground vehicles using the airborne relay does not affect the throughput of the links). It is achieved by considering an airborne relay with multichannel capacity that allows a multi user information exchange as is is presented in [32–34]. It guarantees that every pair of vehicles using air-aided links will be provided with the required throughput while the number of air-aided links does not exceed the capacities of the multichannel airborne relay.

Algorithm 1 Find Optimal Position

```
airborne_relay_positions ← search_region
N ← number of ground vehicles
Q_G_matrix ← 0_{size(search_region)}
for each p_a ∈ airborne_relay_positions do
    T ← 0_{N×N}
    L ← 0_{N×N}
    for i ∈ {1, ..., N} do
        for j ∈ {1, ..., N} − {i} do
            p_i ← position_ground_vehicle_i
            p_j ← position_ground_vehicle_j
            T^{gg} ← T_{gg}(p_i, p_j)
            T^{gag} ← T_{gag}(p_i, p_a, p_j)
            [T]_{ij} ← max(T^{gg} , T^{gag})
        end for
        [L]_{ii} ← 1
    end for
    for i ∈ {1, ..., N} do
        T_i = ∑_{k≠i, v_k∈V} [T]_{ik}
        for j ∈ {1, ..., N} − {i} do
            T_j = ∑_{k≠j, v_k∈V} [T]_{jk}
            [L]_{ij} = −[T]_{ij} / sqrt(T_i T_j)
        end for
    end for
    EIG ← sort(eigenvalues(L))
    λ_2 = EIG(2)
    [Q_G_matrix]_{index(p_a)} ← T_G λ_2
end for
index_Q_G_max ← index(max(Q_G_matrix))
optimal_p_a ← [search_region]_{index_Q_G_max}
return optimal_p_a , max(Q_G_matrix)
```

In Algorithm 1, for each position of the airborne relay, the ground-ground and ground-air-ground throughput are computed for each pair of ground vehicles. Thus, the maximum throughput of each link is selected and used to compute $L(\mathcal{G})$. Then, the second smallest eigenvalue $\lambda_2(\mathcal{G})$ of $L(\mathcal{G})$ and the expected throughput $T_{\mathcal{G}}$ of all the communication links are computed. Thus, $\mathcal{Q}_{\mathcal{G}}$ is computed for each position of the airborne relay in the search region. These values are stored in a matrix with the same size as the matrix representation of the search region. After computing $\mathcal{Q}_{\mathcal{G}}$ for each position and storing the values in a matrix, the maximum element of this matrix and its corresponding index are obtained. Using this index, the corresponding element in the matrix representation of the search region can be retrieved. It corresponds to the airborne relay's position producing the maximum $\mathcal{Q}_{\mathcal{G}}$ in such region. When this region is chosen correctly, that position is the optimal position of the airborne relay.

In Algorithm 1, it can be observed that the right selection of the search region is essential to find the optimal position of the airborne relay, otherwise a local solution different to the optimal position could be obtained. A first approach to define this region can be defining an enough big search region with a low resolution (big size steps) to obtain a first candidate region and then reducing its size and increasing its resolution (small size steps) until finding a good approximation of the optimal airborne relay's position. To improve this approach, the selection of the search region can be made based on the results of Sec. 4.

A lower bound for the height at which the airborne relay could be deployed can be obtained using results of Eq. (4.3) and Eq. (4.6) depending on the obstacles' height distribution considered. For any pair of ground vehicles located at a distance g apart, and a given LoS probability, the height of the airborne relay must satisfy $g < c_u$ or $g < c_t$ depending on the distribution of the obstacles' heights. Links with high throughput (required for high values of $\mathcal{Q}_{\mathcal{G}}$ require a balance between high LoS probability and high capacity. Therefore, the airborne relay's positions producing high $\mathcal{Q}_{\mathcal{G}}$ should produce high LoS probabilities too. If a low value of LoS probability is chosen, the conditions of $g < c_u$ or $g < c_t$ can be used to determine the minimum height of the airborne relay producing that low value of LoS probability. Thus, the airborne relay should be deployed always above that height to ensure a higher LoS probability that will be required for a big throughput. The distance between the furthest ground vehicles from each other can be used in this calculation. It will produce the minimum height that will guarantee to all vehicles have a LoS probability equal to or greater than such low value when the ground-air links are considered. This height can be selected as the lower bound for the height in the search region.

To determine an approximation of the search region in the ground plane onto which the optimal position of the airborne relay is located, the expression in Eq. (4.9) can be used. From Eq. (4.9), it can be observed that for fixed values of h_a, the positions of the airborne relay onto the ground plane producing fixed values of throughput of a ground-air-ground link are contours around the position of the ground vehicles as it is observed in Fig. 4.5. A throughput higher that such fixed value can be obtained only when the airborne relay is deployed over a position inside the region enclosed by the contours. If more than two vehicles are considered, deploying the airborne relay above the intersection of the regions produced by considering each pairwise link will produce a higher throughput for all the ground-air-ground links. Fig. 5.1 shows the regions over the ground plane in which the throughput of each ground-air-ground link is greater than the throughput of the direct link between each pair of vehicles. It is observed that the centroid of the ground vehicles' positions is inside the intersection of such regions. Then, the search region of Algorithm 1 should include the region close to the centroid of the ground vehicles since it is likely that the optimal airborne relay's positions is inside it.

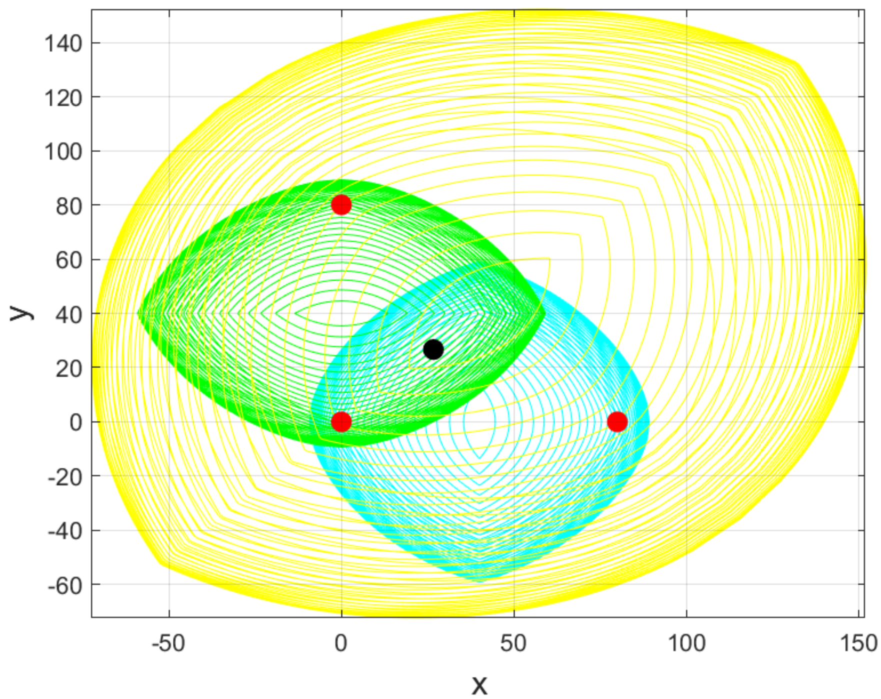

Figure 5.1: Contours of the airborne relay's positions producing constant values of throughput for each ground-air-ground link between three ground vehicles a, b, and (represented by the red dots), located at $(0, 0)$, $(80, 0)$, and $(0, 80)$, respectively. Blue, green, and yellow contours correspond to the links between the pair of vehicles ab, ac, and bc, respectively. The size of the region containing every set of contours is given by the the throughput of the ground-ground link for each pair of vehicles. The black dot represents the centroid of the positions of the ground vehicles.

5.3 Numerical Results

This section presents the numerical results of applying the methods presented in the previous chapters to aid the communication of a network of N ground vehicles. It is assumed that the airborne relay is deployed over the entire workspace of the ground vehicles for calculating the positions that maximize $\mathcal{Q}_{\mathcal{G}}$ using the results presented in Chapter 5. The same parameters mentioned in Sec. 4.3 are considered to calculate the throughput. The uniform distribution is used to describe the obstacles' heights.

5.3.1 Network of Three Ground Vehicles

When the number of ground vehicles increases, for example, $N = 3$, and the vehicles are located at $(0, 0)$, $(60, 0)$, and $(0, 60)$, using Algorithm 1, the position producing the maximum $\mathcal{Q}_{\mathcal{G}} = 150.5$ is found to be $(30, 30, 46)$. If the airborne relay is located at any position in the surface shown in Fig. 5.2, the air-aided communication will provide a value of $\mathcal{Q}_{\mathcal{G}}$ higher than the one obtained when no airborne relay is considered. This surface shows the height of the airborne relay producing the best $\mathcal{Q}_{\mathcal{G}}$ for each position onto the ground plane, being $(30, 30, 46)$ the position producing the maximum $\mathcal{Q}_{\mathcal{G}}$ among all the positions. The outer contour in the ground plane of Fig. 5.2 shows the limit of the region onto which air-aided communication offers better performance when compared with direct-hop communication. The points of the surface located above this contour produce a value of $\mathcal{Q}_{\mathcal{G}} = 95.4$ for the air-aided communication. This value is equal to the value obtained when only direct-hop communication is considered.

Fig. 5.3 shows the behavior of $\mathcal{Q}_{\mathcal{G}}$ as the airborne relay moves above the ground plane with different heights. It can be observed that for all the positions that are above the region outside the outer contour in the ground plane of Fig. 5.3, the airborne relay is unable to improve the communication performance of the system. In that region, $\mathcal{Q}_{\mathcal{G}}$ is constant and equal to 95.4 since none of the positions in such region provide a better performance than the direct-hop communication.

5.3.2 Network of Ten Ground Vehicles

When $N = 10$, and the position of the ground vehicles is as shown in Fig. 5.4 and Fig. 5.5, Algorithm 1 allows to determine that the optimal position for deploying the airborne relay is $(-4, -4.5, 60.5)$. At this position $\mathcal{Q}_{\mathcal{G}} = 52.9$. Fig. 5.4 shows the positions at which the airborne relay could be deployed to aid the communication of the ground vehicles. Also, in Fig. 5.5,

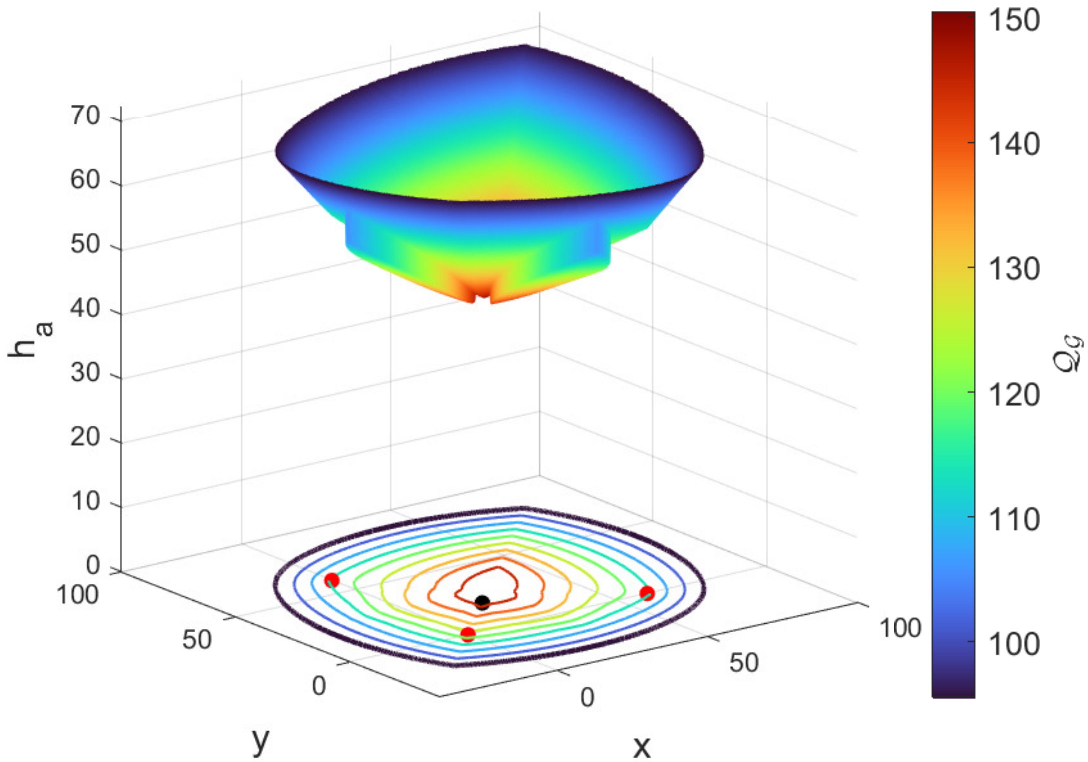

Figure 5.2: Positions of the airborne relay maximizing $\mathcal{Q}_{\mathcal{G}}$ for a system of 3 ground vehicles with respect to the height h_a of the airborne relay for each xy-position.Red dots indicate the position of the ground vehicles and the black dot the centroid of such positions. The color of the surface indicates the value of $\mathcal{Q}_{\mathcal{G}}$.

it can be observed that deploying the airborne relay above regions outside the outer contour in the ground plane will no improve the communication of the system. In these regions $\mathcal{Q}_{\mathcal{G}} = 17.5$ (value obtained when only direct-hop communication is considered). An improvement is possible only when the airborne relay is deployed above the region enclosed by such contour. Above this region, the value of $\mathcal{Q}_{\mathcal{G}}$ can increase up to achieve its maximum value of 52.9.

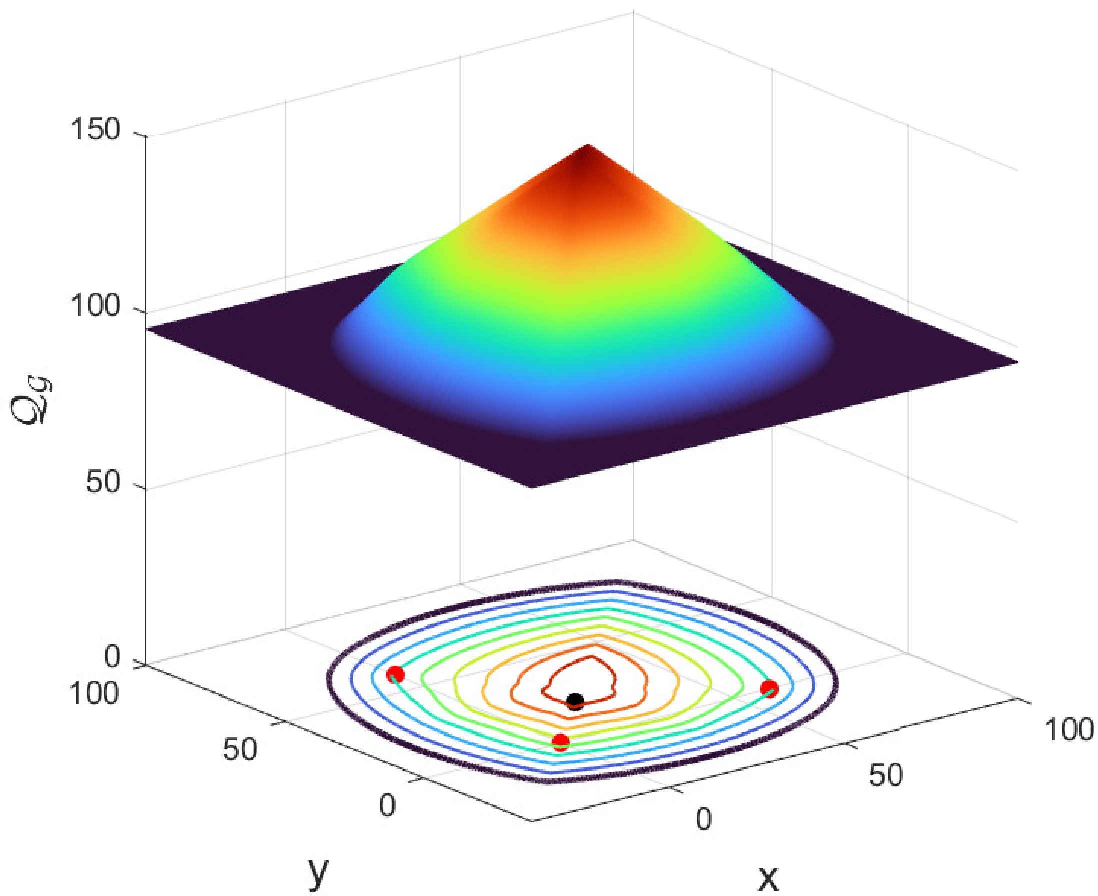

Figure 5.3: $\mathcal{Q}_{\mathcal{G}}$ as a function of the airborne relay's position onto the ground plane and the optimal height for each position. Red dots indicate the position of the ground vehicles and the black dot the centroid of such positions. The color of the surface indicates the value of $\mathcal{Q}_{\mathcal{G}}$.

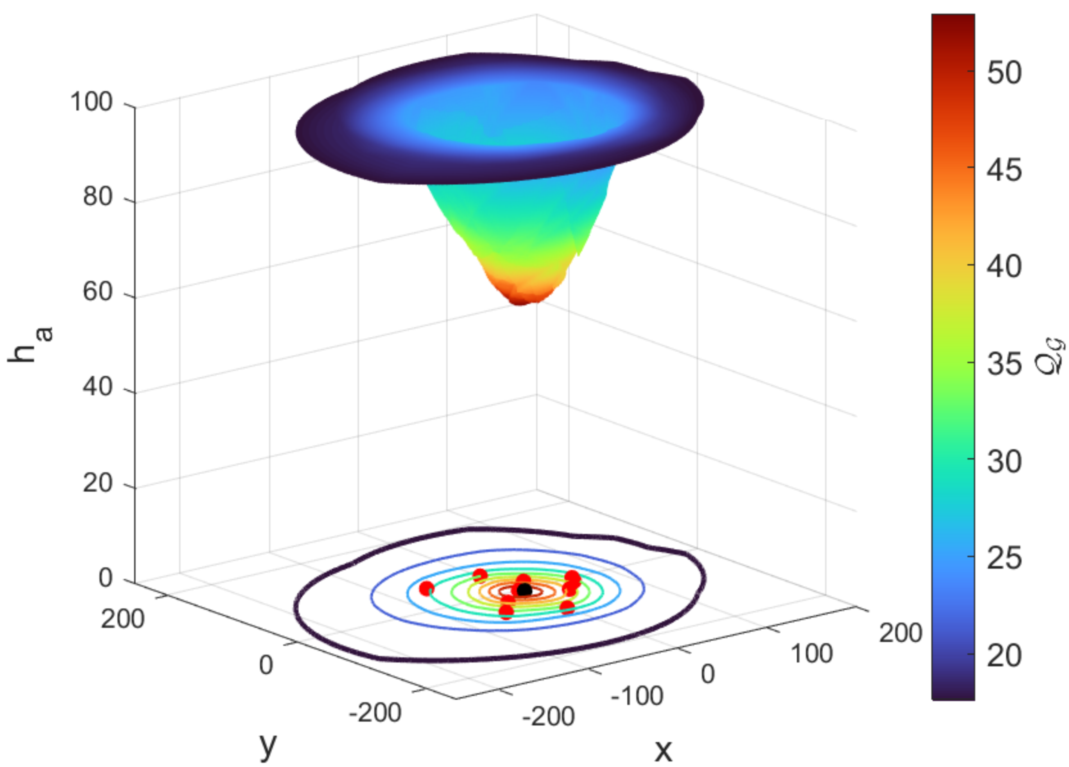

Figure 5.4: Positions of the airborne relay maximizing $\mathcal{Q}_{\mathcal{G}}$ for a system of 10 ground vehicles with respect to the height h_a of the airborne relay for each xy-position. Red dots indicate the position of the ground vehicles and the black dot the centroid of such positions. The color of the surface indicates the value of $\mathcal{Q}_{\mathcal{G}}$.

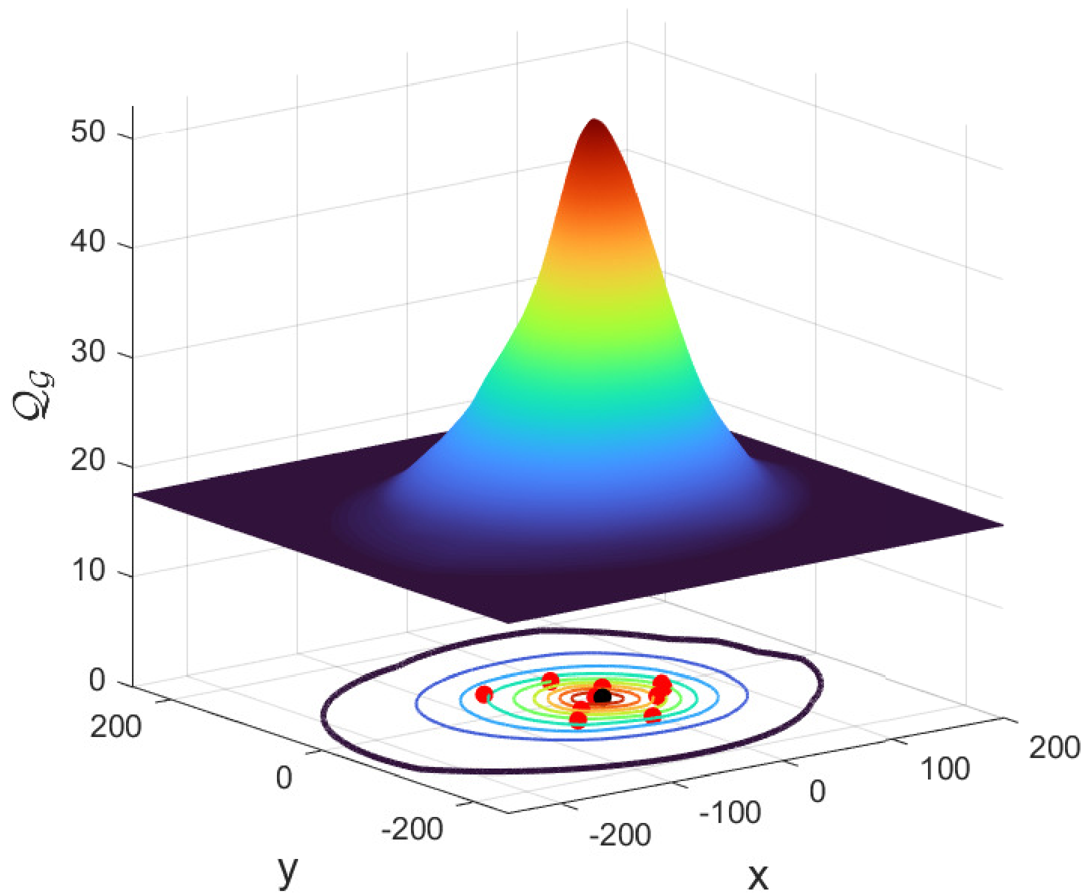

Figure 5.5: $\mathcal{Q}_{\mathcal{G}}$ as a function of the airborne relay's position onto the ground plane and the optimal height for each position. Red dots indicate the position of the ground vehicles and the black dot the centroid of such positions. The color of the surface indicates the value of $\mathcal{Q}_{\mathcal{G}}$.

Chapter 6

Conclusion

6.1 Summary

This thesis considered the air-aided communication of teams of ground vehicles using an air vehicle as an airborne relay. The ground vehicles are deployed in a cluttered environment with obstacles with randomized positions and heights. Due to only obstacles taller than a critical height can block the LoS, the positions of the blockages were modeled by an inhomogeneous PPP.

When mmWave communication or optical devices are considered, the vehicles require a clear line of sight path to communicate. Therefore, an analytical framework was developed to evaluate the impact of the positions of the obstacles and their heights in the LoS. Also, to evaluate the effect of the transmission distance, the throughput was defined. It is a metric that balances the effect of LoS probability and transmission distance on the quality of the communication links. The results obtained with the analytical framework were illustrated with simulations considering two obstacle's height distributions. Truncated Gaussian and uniform.

The first step to determine the optimal position to deploy the airborne relay was to study the case in which only two ground vehicles were considered. In this case, the impact of the distance between ground vehicles and the height of the airborne relay on the LoS probability and throughput were calculated. Also, the positions of the airborne relay producing constant LoS probability and throughput were found and closed-form expressions were provided. Then, these results were extended to the case in which multiple ground vehicles were considered.

Since the throughput was defined as a metric to determine the quality of the link between two vehicles, and not for multiple links, when more than two ground vehicles were considered, a new metric to determine the quality of the communication needed to be defined. This metric was defined using the overall throughput of the network $T_{\mathcal{G}}$ and its connectivity (measured via the second smallest eigenvalue $\lambda_2(\mathcal{G})$ of the graph Laplacian of the network).

When more than two ground vehicles are considered, providing closed-form expressions to determine the optimal position of the airborne relay can be difficult. Therefore, an algorithm that searches for the position producing the greatest value of $\mathcal{Q}_{\mathcal{G}} = T_{\mathcal{G}}\lambda_2(\mathcal{G})$ was designed. This algorithm used the theoretical results presented in the thesis to determine such a position.

To achieve the optimal position, the search algorithm calculates $\mathcal{Q}_{\mathcal{G}} = T_{\mathcal{G}}\lambda_2(\mathcal{G})$ for each position on the search region. To increase the convergence time of the algorithm, the search region is bounded according to the results obtained in Chapter 4, where positions producing constant values of LoS probability and throughput are calculated. It is found that the optimal position should be over a region in the $x - y$ plane enclosing the centroid of the ground vehicles' positions. Once the search region is established, the search algorithm can be used to determine the optimal position. This position will provided the maximum value of $\mathcal{Q}_{\mathcal{G}}$ among all the other positions. Deploying the airborne relay in this positions will offer the best balance between overall throughput and connectivity to the network.

6.2 Conclusion

The results of this thesis allow us to determine the optimal position to deploy an airborne relay when it is required to aid the communication of two or more ground vehicles. For the case of two ground vehicles, it is found that the optimal position is above the middle of the ground vehicles. However, depending on the type of air vehicle used, it could be difficult to maintain the air vehicle in a fixed position (for example if a fixed-wing aircraft is used). In this case, our results provide the regions in the 3-D space in which the air vehicle could move while the desired communication quality is guaranteed. These results are then extended to the case of multiple ground vehicles, in which the optimal position or the positions producing fixes values of $\mathcal{Q}_{\mathcal{G}}$ are provided. The positions to deploy the air vehicle depend on the obstacle's height distributions.

When different height distributions are considered, a similar effect is observed independently of the type of height distributions. As the distance between ground vehicles increases, the height of the airborne relay needs to be increased to provide the same value of LoS probability. However, as the height of the airborne relay increases, the channel capacity of the links decreases. Since the throughput is a metric that balances both LoS probability and capacity, the positions producing high values of throughput need to find a balance between high LoS and high capacity.

When the number of ground vehicles and their separation distances increases, the positions that balance LoS and capacity produce low values of throughput and therefore low values of $\mathcal{Q}_{\mathcal{G}}$. It can be observed in the results for 3 and 10 ground vehicles. The value of $\mathcal{Q}_{\mathcal{G}}$ is smaller when 10 vehicles are considered. For this case, deploying multiple airborne relays could be useful.

6.3 Future Work

As the number of ground vehicles and their separation distances increase, the aid of only one airborne relay could not be enough to guarantee the desired communication performance. In this case, as future work, it is proposed to analyze how to deploy multiple airborne relays. The results presented in this thesis are a gateway to determine the optimal positions of the multiple airborne relays. Given the number of ground vehicles in the $x-y$ plane and the desired communication performance, the results of this thesis can be extended to determine the set of ground vehicles that can be assisted by a specific airborne relay. For example the vehicles on certain regions of the $x - y$ plane. Then, multiple airborne relays can be deployed to aid the ground vehicles in different regions of the $x - y$ plane. Since the LoS probability does not affect the communication links between airborne relays, the throughput of the airborne-to-airborne links will depend only on their capacities (*i.e.*, it depends only on their separation distances).

References

[1] J. Langelaan and S. Rock, "Towards autonomous UAV flight in forests," in *AIAA Guidance, Navigation, and Control Conference and Exhibit*, 2005, p. 5870.

[2] X. Zheng, S. Koenig, D. Kempe, and S. Jain, "Multirobot forest coverage for weighted and unweighted terrain," *IEEE Transactions on Robotics*, vol. 26, no. 6, pp. 1018–1031, 2010.

[3] K. Harikumar, J. Senthilnath, and S. Sundaram, "Multi-UAV oxyrrhis marina-inspired search and dynamic formation control for forest firefighting," *IEEE Transactions on Automation Science and Engineering*, vol. 16, no. 2, pp. 863–873, 2018.

[4] M. S. Couceiro, D. Portugal, J. F. Ferreira, and R. P. Rocha, "Semfire: Towards a new generation of forestry maintenance multi-robot systems," in *2019 IEEE/SICE International Symposium on System Integration (SII)*. IEEE, 2019, pp. 270–276.

[5] Y. Tian, K. Liu, K. Ok, L. Tran, D. Allen, N. Roy, and J. P. How, "Search and rescue under the forest canopy using multiple UAVs," *The International Journal of Robotics Research*, vol. 39, no. 10-11, pp. 1201–1221, 2020.

[6] L. F. Oliveira, A. P. Moreira, and M. F. Silva, "Advances in forest robotics: A state-of-the-art survey," *Robotics*, vol. 10, no. 2, p. 53, 2021.

[7] B. Grocholsky, J. Keller, V. Kumar, and G. Pappas, "Cooperative air and ground surveillance," *IEEE Robotics & Automation Magazine*, vol. 13, no. 3, pp. 16–25, 2006.

[8] L. Chaimowicz, A. Cowley, D. Gomez-Ibanez, B. Grocholsky, M. Hsieh, H. Hsu, J. Keller, V. Kumar, R. Swaminathan, and C. Taylor, "Deploying air-ground multi-robot teams in urban environments," in *Multi-Robot Systems. From Swarms to Intelligent Automata Volume III:*

Proceedings from the 2005 International Workshop on Multi-Robot Systems. Springer, 2005, pp. 223–234.

[9] M. Wei and V. Isler, "Air to ground collaboration for energy-efficient path planning for ground robots," in *Proc. IEEE/RSJ International Conference on Intelligent Robots and Systems (IROS)*, 2019, pp. 1949–1954.

[10] R. Doriya, S. Mishra, and S. Gupta, "A brief survey and analysis of multi-robot communication and coordination," in *International Conference on Computing, Communication & Automation*. IEEE, 2015, pp. 1014–1021.

[11] E. Hriba, M. C. Valenti, K. Venugopal, and R. W. Heath, "Accurately accounting for random blockage in device-to-device mmwave networks," in *GLOBECOM 2017-2017 IEEE Global Communications Conference*. IEEE, 2017, pp. 1–6.

[12] M. F. Mysorewala, D. O. Popa, and F. L. Lewis, "Multi-scale adaptive sampling with mobile agents for mapping of forest fires," *Journal of Intelligent and Robotic Systems*, vol. 54, no. 4, pp. 535–565, 2009.

[13] B. Benjamin, G. Erinc, and S. Carpin, "Real-time wifi localization of heterogeneous robot teams using an online random forest," *Autonomous robots*, vol. 39, no. 2, pp. 155–167, 2015.

[14] A. Gasparetto, P. Boscariol, A. Lanzutti, and R. Vidoni, "Path planning and trajectory planning algorithms: A general overview," *Motion and operation planning of robotic systems*, pp. 3–27, 2015.

[15] F. Baccelli and X. Zhang, "A correlated shadowing model for urban wireless networks," in *2015 IEEE Conference on Computer Communications (INFOCOM)*. IEEE, 2015, pp. 801–809.

REFERENCES

[16] M. Gapeyenko, D. Moltchanov, S. Dmitri, and R. W. Heath Jr, "Line-of-sight probability for mmwave-based UAV communications in 3D urban grid deployments," *IEEE Transactions On Wireless Communications*, vol. 20, no. 10, pp. 6566–6579, 2021.

[17] E. Hriba, M. C. Valenti, and R. W. Heath, "Optimization of a millimeter-wave UAV-to-ground network in urban deployments," in *MILCOM 2021-2021 IEEE Military Communications Conference (MILCOM)*. IEEE, 2021, pp. 861–867.

[18] S. Karaman and E. Frazzoli, "High-speed flight in an ergodic forest," in *2012 IEEE International Conference on Robotics and Automation*. IEEE, 2012, pp. 2899–2906.

[19] ——, "High-speed motion with limited sensing range in a poisson forest," in *2012 IEEE 51st IEEE Conference on Decision and Control (CDC)*. IEEE, 2012, pp. 3735–3740.

[20] B. Martinez R and G. A. Pereira, "Fast path computation using lattices in the sensor-space for forest navigation," in *2021 IEEE International Conference on Robotics and Automation (ICRA)*. IEEE, 2021, pp. 1117–1123.

[21] T. Kohyama and T. Hara, "Frequency distribution of tree growth rate in natural forest stands," *Annals of Botany*, vol. 64, no. 1, pp. 47–57, 1989.

[22] J. M. Felfili, "Diameter and height distributions in a gallery forest tree community and some of its main species in central brazil over a six-year period (1985-1991)," *Brazilian Journal of Botany*, vol. 20, no. 2, pp. 155–162, 1997.

[23] F. Mauro, R. Valbuena, J. Manzanera, and A. García-Abril, "Influence of global navigation satellite system errors in positioning inventory plots for tree-height distribution studies," *Canadian journal of forest research*, vol. 41, no. 1, pp. 11–23, 2011.

[24] J. D. Pabon, S. Alkandari, M. C. Valenti, and X. Yu, "Air-aided communication between ground assets in a Poisson forest," in *Proc. IEEE Military Communications Conference (MILCOM)*, 2022, pp. 133–139.

[25] J. D. Pabon, M. C. Valenti, and X. Yu, "Where to deploy an airborne relay in unknown environments: Feasible locations for throughput and los enhancement," in *Proc. IEEE Military Communications Conference (MILCOM)*, 2023.

[26] E. Hriba and M. Valenti, "Correlated blocking in mmwave cellular networks: Macrodiversity, outage, and interference," *Electronics*, vol. 8, no. 10, article number 1187, Oct. 2019.

[27] I. S. Gradshteyn and I. M. Ryzhik, *Table of Integrals, Series, and Products*. Academic press, 2014.

[28] T. S. Rappaport, S. Sun, R. Mayzus, H. Zhao, Y. Azar, K. Wang, G. N. Wong, J. K. Schulz, M. Samimi, and F. Gutierrez, "Millimeter wave mobile communications for 5G cellular: It will work!" *IEEE Access*, vol. 1, pp. 335–349, 2013.

[29] Y. Rahayu and M. I. Hidayat, "Design of 28/38 GHz dual-band triangular-shaped slot microstrip antenna array for 5G applications," in *International Conference on Telematics and Future Generation Networks (TAFGEN)*, 2018, pp. 93–97.

[30] F. R. Chung, *Spectral Graph Theory*. American Mathematical Society, 1997, vol. 92.

[31] M. Mesbahi and M. Egerstedt, *Graph Theoretic Methods in Multiagent Networks*, 2010.

[32] N. H. Mahmood, D. Laselva, D. Palacios, M. Emara, M. C. Filippou, D. M. Kim, and I. de-la Bandera, "Multi-channel access solutions for 5G new radio," in *2019 IEEE Wireless Communications and Networking Conference Workshop (WCNCW)*, 2019, pp. 1–6.

REFERENCES

[33] B. Mughal, Z. M. Fadlullah, M. M. Fouda, and S. Ikki, "Allocation schemes for relay communications: A multiband multichannel approach using game theory," *IEEE Sensors Letters*, vol. 6, no. 1, pp. 1–4, 2022.

[34] H. Lee, S. Lee, and Y. Ko, "Multichannel relay assisted noma-aloha with reinforcement learning based random access," in *2023 IEEE 97th Vehicular Technology Conference (VTC2023-Spring)*, 2023, pp. 1–5.